Environ Geol (2006) 50: 1151–1170
DOI 10.1007/s00254-006-0288-z

ORIGINAL ARTICLE

J. J. Gómez
J. Lillo
B. Sahún

Naturally occurring arsenic in groundwater and identification of the geochemical sources in the Duero Cenozoic Basin, Spain

Received: 16 February 2006
Accepted: 29 March 2006
Published online: 17 May 2006
© Springer-Verlag 2006

J. J. Gómez (✉)
Departamento de Estratigrafia,
Instituto de Geologia Economica
(CSIC-UCM), Facultad de Ciencias
Geologicas, Universidad Complutense,
28040 Madrid, Spain
E-mail: jgomez@geo.ucm.es
Tel.: +34-91-3944783
Fax: +34-91-3944808

J. Lillo
Area de Geologia, Escuela Superior de
Ciencias Experimentales y Tecnologia,
Universidad Rey Juan Carlos,
Tulipan s/n., 28993 Mostoles, Spain

B. Sahún
Direccion General de Obras Hidraulicas y
Calidad de las Aguas, Ministerio de
Medio Ambiente, Plaza de San Juan de la
Cruz, s/n., 28003 Madrid, Spain

Abstract Arsenic concentrations surpassing potability limit of 10 μg/L in the groundwater supplies of an extensive area in the Duero Cenozoic Basin (central Spain) have been detected and the main sources of arsenic identified. Arsenic in 514 samples of groundwater, having mean values of 40.8 μg/L, is natural in origin. Geochemical analysis of 553 rock samples, assaying arsenic mean values of 23 mg/kg, was performed. Spatial coincidence between the arsenic anomaly in groundwater and the arsenic lithogeochemical distribution recorded in the Middle Miocene clayey organic-rich Zaratan facies illustrates that the rocks of this unit are the main source of arsenic in groundwater. The ferricretes associated to the Late Cretaceous–Middle Miocene siliciclastics also constitute a potential arsenic source. Mineralogical study has identified the presence of arsenic in iron oxides, authigenic pyrite, manganese oxides, inherited titanium–iron oxides, phyllosilicates and organomineral compounds. Arsenic mobilization to groundwater corresponds to arsenic desorption from iron and manganese oxides and from organic matter.

Keywords Arsenic · Groundwater quality · Sedimentary rocks · Hydrochemistry · Cenozoic · Duero Basin · Spain

Introduction

The presence of arsenic in groundwater in pernicious concentrations for human health constitutes a worldwide high-priority groundwater quality problem (Duker et al. 2005). In many areas of the world, arsenic in the environment can be related to human activities such as base and precious metals mining and smelting, coal combustion, tanning waste, pigment production, pressure-treated wood, increased growth in feedlot-raised poultry and, in the past, to the use of pesticides (Nriagu 1994; Oremland and Stolz 2003). Arsenic pollution from these sources to groundwater tends to be mostly local. However, the main source for contaminating the drinking water aquifers all around the world is the naturally occurring arsenic. This arsenic can be sourced, among other causes, by geothermal and volcanic activities, aquitards mainly composed of clay-rich and/or organic-rich lithologies containing arsenic-rich minerals (e.g. arsenopyrite, pyrite, enargite) or aquifers containing iron and manganese oxides. These oxides show high affinity to arsenic and/or linked with sulphide minerals or organic carbon (Korte 1991; Nriagu 1994; Schreiber et al. 2000; Smedley and Kinninburgh 2002; Stollenwerk 2003).

In Spain, the presence of naturally occurring arsenic in groundwater has been reported in the sedimentary Duero and Tajo Cenozoic basins, located in central

Spain (Fig. 1a). Arsenic occurrences in the Tajo Basin have been studied by Aragonés Sanz et al. (2001), Hernández García and Fernández Ruiz (2002) and Hernández-García and Custodio (2004).

Many arsenic-bearing mineralizations, represented by As, Sb, Au old mining workings and mineral shows (Fig. 1b), are hosted in the Palaeozoic rocks that surround the Duero Basin. Local arsenic pollution in groundwater, related to W, Sn (As) old mines, hosted in intrusive and metamorphic rocks west of the Salamanca town, has been reported (García-Sánchez and Álvarez-Ayuso 2003).

In the Duero Cenozoic Basin, whose main geological features are shown in Fig. 1b, the presence of arsenic in concentrations that largely surpass the potability limits has been detected. This pollution affects the groundwater used for drinking purposes in several townships of the Avila, Segovia and Valladolid provinces (Barroso et al. 2002; Moyano et al. 2002; Calvo Revuelta et al. 2003; Sahún et al. 2003, 2004a, b; Carretero Rivera et al. 2004; García-Sánchez et al. 2005). The affected area, whose boundaries are represented in Fig. 2, exceeds 4,000 km^2.

The main objectives of this work are to outline and characterize the geological, geochemical and mineralogical features of the area where the arsenic concentration makes groundwater unfit for human drinking, to determine the source of arsenic and finally to know the mineralogical species as well as the geochemical processes that intervene in the arsenic mobilization and incorporation to the groundwater. The aim of the stratigraphic, sedimentological and geochemical studies was to determine the arsenic concentration of the different stratigraphic intervals that potentially contribute to the presence of arsenic in groundwater.

Materials and methods

To reach the proposed goals, hydrochemical, lithogeochemical, sedimentological and mineralogical studies were performed in the area of interest.

The hydrochemical study, which was restricted to the eastern area (Fig. 2), was planned from the analytical results obtained from the Consejeria de Salud of the Junta de Castilla y Leon and from the Confederacion Hidrografica del Duero from wells and springs waters.

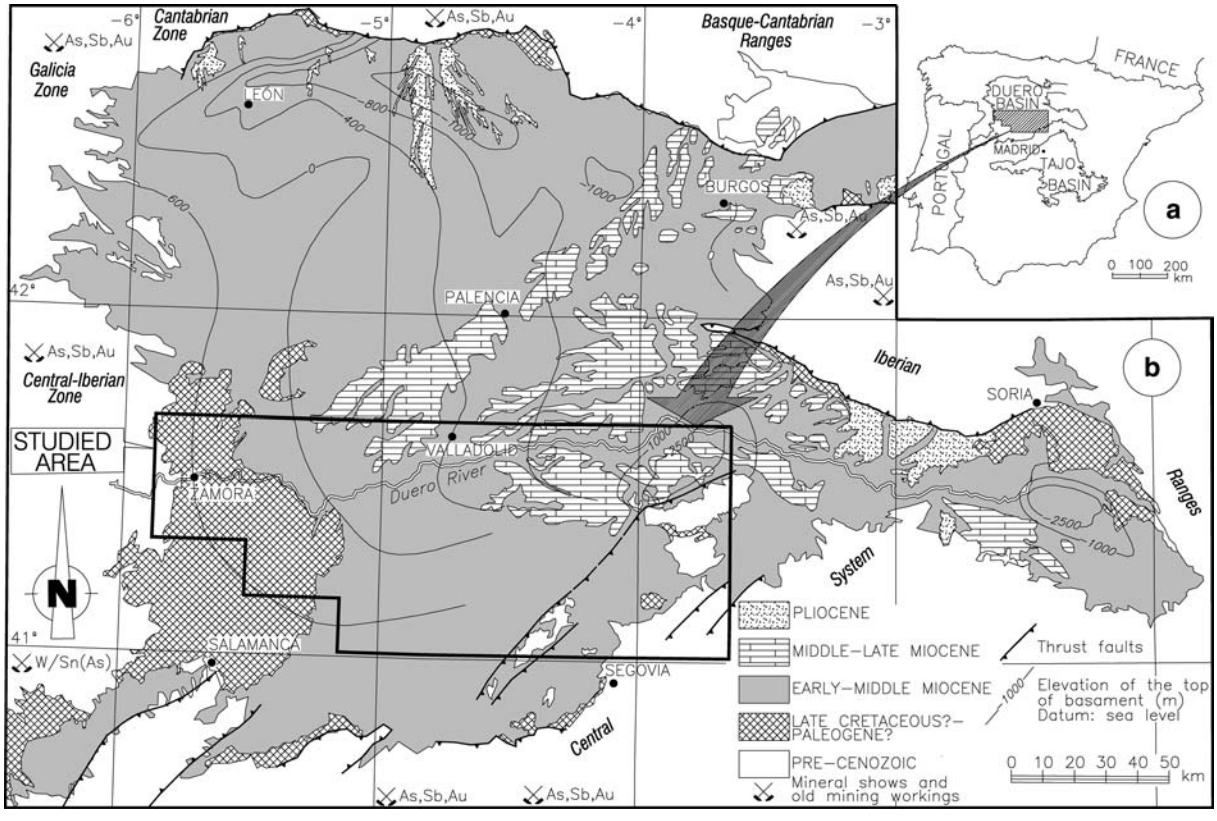

Fig. 1 **a** Location of the Duero and Tajo Cenozoic basins in Spain. **b** Geological map of the Duero Basin, modified from the 1:2,000,000 scale Geologic and Tectonic Maps of Spain (IGME-SGE 2004) and location of the studied area. The age of the oldest materials that fill up the Duero Basin have been attributed to the Palaeocene, according to the mentioned map, and also to the late Cretaceous, according to Pol et al. (1992) and Alonso-Gavilán et al. (2004). The names of the surrounding mountainous systems and the mineral ores containing arsenic are also indicated

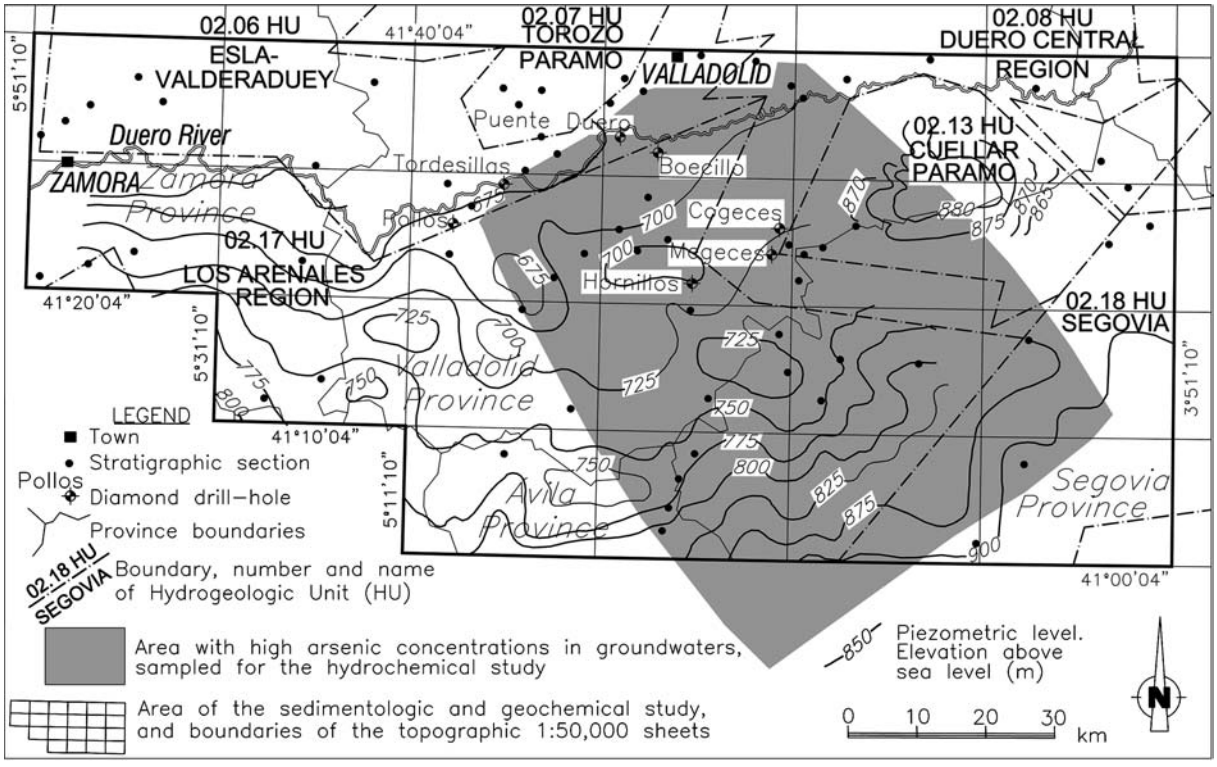

Fig. 2 Location of the area with arsenic anomalies in groundwater, the area of the sedimentological study, location of the measured stratigraphic sections and drill holes, which have been sampled for geochemical studies, and the province and hydrogeological units boundaries. Contours of the elevation of the piezometric levels were modified from Sahún (1991, 2002)

In the study, two water sampling surveys in wells and springs were carried out, with a total of 514 water samples being collected. The first survey was carried out during September and October 2000 (at the end of the summer dry season), to obtain the first evaluation of the arsenic concentration and its spatial distribution. This sampling survey revealed the situation at the end of the hydrological year, after the irrigation period, under low water level conditions. In this survey, a total of 384 samples were collected (315 samples of groundwater, from which 215 were collected in deep wells, 84 in shallow wells and 16 in springs) and 42 samples of superficial waters.

The second sampling survey was carried out during April and May 2001 (at the end of the rainy period, under high water level conditions), to evaluate the arsenic variations in the sampling sites where the highest concentrations were recorded. The area covered by the second survey was similar to the previous one, although the number of sampled sites was smaller. A total of 157 sites (114 deep wells, 31 shallow wells and 11 springs and 1 superficial water) were sampled.

The 514 water samples were analysed for 67 elements by inductively coupled plasma-mass spectrometry (ICP-MS). Parameters such as pH, electric conductivity, temperature, dissolved oxygen and redox potential (Eh) were determined in the sampling site, and standard chemical analysis including Na^+, K^+, Ca^{2+}, Mg^{2+}, Cl^-, SO_4^{2-}, HCO_3^-, CO_3^{2-}, NO_3^-, NO_2^-, NH_4^+, Li, B, SiO_2, Fe, Mn and pH, conductivity and total dissolved solids were carried out.

The sedimentologic, geochemical and mineralogical studies were extended to a wider area, of about 11,000 km^2 (Fig. 2), to use the results of the present study as a reference for new unstudied areas that can potentially contain arsenic in groundwater. Three diamond drill holes, with a total accumulated depth of 967 m, were drilled in those areas recording the highest arsenic values in groundwater. After analysis of the available geological and geophysical information, the area of extension of the fieldwork and the stratigraphic units to carry out the sedimentological study were selected. A total of 69 stratigraphic sections with an accumulated thickness of 3,439 m were studied and sampled (Fig. 2), being the previous geological mapping reviewed. Drill cores of 2,053 m from seven holes, drilled by the Direccion General de Obras Hidraulicas y Calidad de las Aguas of the Ministerio de Medio Ambiente, were studied and sampled for geochemical analysis. The total depth of the boreholes is shown in Table 1.

Table 1 Depth of the core holes drilled by the Dirección General de Obras Hidraulicas y Calidad de las Aguas studied and sampled in this work

Drill hole name	Depth (m)
Hornillos	501
Cogeces	206
Megeces	260
Pollos	278
Puente Duero	300
Tordesillas	300
Boecillo	208
Total	2,053

Measurement of 35 elements (As, Au, Ag, Ba, Br, Ca, Co, Cr, Cs, Fe, Hf, Hg, Ir, Mo, Na, Ni, Rb, Sb, Sc, Se, Sn, Sr, Ta, Th, U, W, Zn, La, Ce, Nd, Sm, Eu, Tb, Yb and Lu) in the 553 rock samples from the stratigraphic sections (378 samples) and in the core recovered in the holes (175 samples), was performed by Instrumental Neutron Activation Analysis (INAA). Concentration of major elements as oxides (SiO_2, Al_2O_3, $Fe_2O_{3(total)}$, MnO, MgO, CaO, Na_2O, K_2O, TiO_2 and P_2O_5) in 58 samples with arsenic concentration above 43.5 mg/kg was determined by X-ray fluorescence (XRF).

The concentration of organic carbon in 17 samples was analysed by spectroscopy, to check the relationship between the arsenic concentrations in rocks and the presence of organic matter. A mineralogical study on 131 samples showing arsenic concentration above geochemical background was performed. The study consisted of the petrographic revision of 41 samples by reflected light and transmitted optical microscope, 101 mineralogical determinations by X-ray diffraction (43 on total powder and 58 on oriented aggregates for clays identification) and the study of 18 samples by scanning electronic microscope (SEM) with energy dispersive X-ray (EDX) analysis (87 determinations on powdered samples and polish test-tube preparations).

To know the distribution and variation of the arsenic concentration in the rocks, contour maps of the arithmetical mean values of arsenic concentrations for every one of the considered stratigraphic intervals have been performed. For this purpose, the arithmetic mean of the arsenic values obtained in the samples corresponding to a given interval was assigned to the site of each stratigraphic section or drill hole. In order to simplify the tracing of the contour maps, the value of 25 mg/kg arsenic (instead of the calculated background value of 28.50 mg/kg) has been taken as graphical reference. Contour intervals were traced for every 5 mg/kg arsenic, and the intervals comprising 25 mg/kg arsenic have been hatched. Tracing of the contours has been computer-aided but the results have been checked and corrected manually to avoid inconsistencies, but respecting their mathematical adjustment.

Geological and hydrogeological setting

The Duero Basin is an intraplate continental basin of about 50,000 km^2, which developed from Late Cretaceous until Late Cenozoic. At that time span, the basin acted as a foreland basin of the surrounding Cantabrian Zone and Basque-Cantabrian Range in the north, the Iberian Range in the east and the Central System in the south, which constitute complex fold and thrust belts. These Alpine compressional ranges, constituted by Palaeozoic and Mesozoic rocks, are thrusting, in many cases, the Cenozoic deposits of the Duero Basin, which are virtually undeformed. The Galicia and Central Iberian Zones, which form the western boundary of the basin, seem to represent a relatively passive margin. Arsenic-bearing mineralization, mainly related to antimony and gold and occasionally to tin and tungsten, is hosted by Palaeozoic rocks of the surrounding basin margins. Thickness of the sediments filling up the Duero Basin surpass 2,500 m in the area located between the Iberian Ranges and the Central System, and values above 2,000 m are reached north of Segovia and above 1,000 m east of Leon (Fig. 1b).

The general facies distribution of the basin corresponds to a continental foreland basin model with alluvial fan deposits grading into alluvial plain and evaporitic and carbonated lacustrine environments towards the centre of the basin. Facies distribution and spatial evolution is strongly controlled by the tectonics of the basin boundaries (Colmenero et al. 2001; Armenteros et al. 2002; Alonso-Gavilán et al. 2004).

The complex evolution of the ranges surrounding the basin and the variety of the source rocks resulted in the generation of a multilayered aquifer system. In the area affected by the presence of arsenic in groundwater (Fig. 2), the aquifer system includes part of several hydrogeological units (HU; Navarro et al. 1989) called the Esla–Valderaduey HU (02.02), the Torozo Paramo HU (02.07), the Duero Central Region HU (02.08), the Cuellar Paramo HU (2.13), the Los Arenales Region HU (02.17) and the Segovia HU (02.18) (Fig. 2; Sánchez et al. 1990). Average precipitation values in a large part of the study area are between 400 and 450 mm/year, reaching 1,000 mm/year in the topographically higher areas located south and southeast.

The Los Arenales Region HU is a multilayered anisotrope and heterogeneous aquifer of mainly detrital Cenozoic sediments, that can be free or confined depending on the relative stratigraphic architecture of aquifers and aquitards. It constitutes the biggest regional aquifer, on which most of the well extractions are established. The main water recharge to the aquifer is the infiltration of 228 hm^3/year rainfall (Sahún 2001) and, in natural regime, the main discharge area is the

Duero river, which is the most important drainage element of the basin, and represents the northern boundary of the Los Arenales Region HU. At present, these discharges have decreased due to the pumping of important groundwater volumes (234 hm^3/year; Sahún 2002). Contouring of the water levels in the Los Arenales Region HU shows that regional water flow in the area of anomalous arsenic concentration in groundwater has a south–north orientation (Fig. 2). In three dimensions, there is a descending component in the recharge areas, located to the south and southeast, and a marked upward component in the discharge area in the north of the unit, near the Duero River.

The Duero Central Region HU, formed by Miocene clayey sands and marls, constitutes a nearly 200 m thick aquitard, stratigraphically located above the Los Arenales Region HU aquifer and under the Cuellar Paramo HU.

The Cuellar Paramo HU is a free aquifer constituted by Middle to Late Miocene carbonate rocks, on which the groundwater flows from the centre of the outcrop toward the borders (Fig. 2). Infiltration of rainwater (24 hm^3/year; Sahún 1991) is the main source of recharge. Discharge is made through the springs located towards the boundaries of the outcrop and by pumping (17 hm^3/year; Sahún 2001). Finally, the Segovia HU includes Cenozoic detrital sediments and Cretaceous carbonate rocks (Sánchez et al. 1990).

Hydrochemistry

Results of the chemical and physico-chemical parameters and major and trace elements concentrations from the analysis of the 514 water samples collected in the area of interest are summarized in Table 2.

Groundwater in the studied area is generally Ca–Mg–HCO_3 to Na–HCO_3 type, although Ca–Na–SO_4 type water is also found in some parts of the investigated zone, as shown in Fig. 3. pH is near neutral to alkaline (pH 5.87–10.58, mean 8.1; Table 2). Field-measured redox potential ranges from −187.5 to 374.5 mV (mean 83.08 mV), reflecting a predominately oxic to locally strong reducing character of the aquifer. Major ion composition is dominated by HCO_3^- (29.3–687.1 mg/L, mean 241.25 mg/L) and in lower proportion by SO_4^{2-} (2.3–1,236.0 mg/L, mean 123.3 mg/L). Concentrations of NO_3^- (mean 59.6 mg/L) and Cl^- (mean 65 mg/L) are generally low, except for some locally high occurrences. Sixty-five percent of the 315 samples of groundwater analysed from the first survey exceed the potability limit of 10 μg/L arsenic, set out in the Directive 98/83 of the European Union, applicable to Spain. In the 42 samples of superficial waters no remarkable arsenic concentrations were recorded. The maximum arsenic value (613 μg/L) was obtained in a 40 m deep private well but

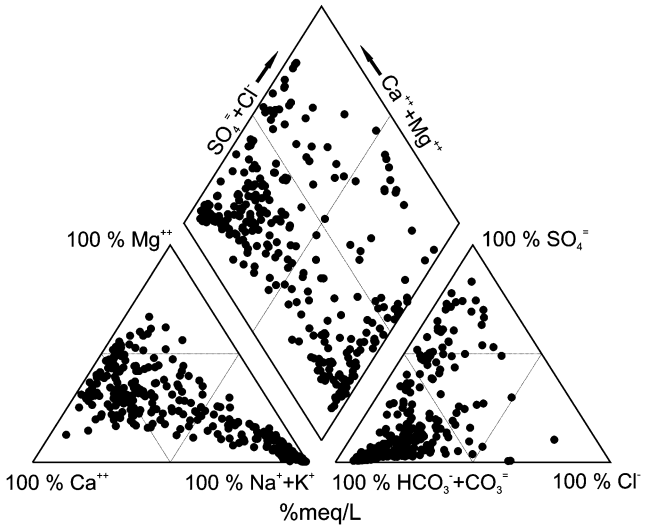

Fig. 3 Piper diagram of the groundwaters in the studied area (samples collected in September–October 2000). Note that they are generally Ca–Mg–HCO_3 to Na–HCO_3 type, although Ca–Na–SO_4 type water is also found

high concentrations were also recorded in several municipal wells used for human supply in the area located south of the Valladolid town (Fig. 2).

Contouring of the arsenic values in the water wells of the studied area is shown in Fig. 4. The contour map shows that a large part of the region has arsenic concentrations in groundwater above the potability limit of 10 μg/L. Concentrations higher than 50 μg/L are located in the northeastern area of the Los Arenales Region HU, and the highest concentrations are in the intersection of that unit with the Cuellar Paramo HU and in the corridor of the Duero Central Region HU.

The analysis of the relationship between the arsenic concentration and the depth of the wells is shown in Fig. 5. This cross-plot reveals a higher arsenic concentration in the 70–100 m depth wells and in the shallow wells collared at an elevation between 700 and 800 m above sea level in the southwestern border of the Cuellar Paramo HU, coinciding with the outcrops of a clayey organic-rich stratigraphic unit. However, arsenic concentrations in wells relatively close to each other and of similar depth are very different. In contrast, high arsenic concentrations are recorded in wells of very different depths and collared at different elevations. High values of arsenic are not observed in the deepest wells that presumably would capture waters of a longer residence time in the aquifer. In fact, the highest arsenic values are recorded in wells shallower than 100 m depth (Fig. 5), indicating some stratigraphic control as will be discussed later on. Arsenic spatial distribution in the groundwater is not uniform, neither in a map (Fig. 4) nor at depth (Fig. 5). In addition, a progressive enrichment in the south–north direction of the regional

Table 2 Summary of chemical and physico-chemical parameters and major and trace elements concentrations of the water samples

	Min	Max	Mean	SD	10th P	90th P
pH	5.87	10.58	8.113	0.936	7.184	9.546
Conductivity (μS/cm)	2.12	3,680.00	799.784	649.744	277.000	1,681.600
Temperature (°C)	8.00	23.00	15.761	2.521	13.000	19.260
O_2 (mg/L)	−1.80	11.90	3.825	2.123	1.200	6.128
Eh (mV)	−187.50	374.50	83.079	73.264	−9.980	175.830
Cl^- (mg/L)	9.90	1,099.00	65.054	94.998	17.000	136.100
SO_4^{2-} (mg/L)	2.30	1,236.00	123.365	226.500	4.730	438.370
HCO_3^- (mg/L)	29.30	687.10	241.255	97.027	134.200	370.640
CO_3^{2-} (mg/L)	0.00	177.00	6.376	15.020	0.000	25.800
NO_3^- (mg/L)	0.00	544.10	59.592	86.870	3.600	177.500
Na^+ (mg/L)	4.00	901.80	93.210	116.299	10.910	231.790
Mg^{2+} (mg/L)	0.20	186.50	29.972	35.031	1.290	79.090
Ca^{2+} (mg/L)	1.20	423.20	58.800	62.545	3.200	134.580
K^+ (mg/L)	0.10	73.10	3.727	5.849	0.500	7.940
NO_2^- (mg/L)	0.00	2.75	0.042	0.199	0.000	0.060
NH_4 (mg/L)	0.00	0.79	0.016	0.069	0.000	0.030
B (mg/L)	0.00	2.00	0.049	0.125	0.000	0.110
P (mg/L)	0.16	17.00	3.770	2.755	1.245	7.527
SiO_2 (mg/L)	4.38	84.76	23.469	14.450	9.782	42.684
Li (μg/L)	1.16	504.63	65.780	75.946	12.638	145.347
Be (μg/L)	BDL	0.10	–	–	–	–
Al (μg/L)	BDL	598.16	6.148	47.504	0.000	8.338
Sc (μg/L)	1.58	31.08	6.335	3.973	3.108	10.494
Ti (μg/L)	1.40	24.72	5.921	3.941	2.584	10.343
V (μg/L)	0.48	248.86	19.794	29.742	2.390	50.223
Cr (μg/L)	BDL	31.19	2.616	5.027	0.000	6.263
Mn (μg/L)	BDL	868.67	5.587	52.394	0.000	2.789
Fe (μg/L)	BDL	569.88	28.645	83.819	0.000	98.044
Co (μg/L)	BDL	3.16	0.067	0.267	0.000	0.127
Ni (μg/L)	BDL	89.70	4.401	9.308	0.000	10.602
Cu (μg/L)	BDL	11.20	1.286	1.781	0.000	3.505
Zn (μg/L)	BDL	9,560.00	50.282	550.998	0.000	24.045
Ga (μg/L)	BDL	0.38	0.019	0.055	0.000	0.087
Ge (μg/L)	BDL	0.77	0.115	0.132	0.000	0.283
As (μg/L)	0.42	613.45	40.831	65.842	3.153	113.619
Se (μg/L)	BDL	20.02	1.735	2.212	0.233	3.882
Br (μg/L)	BDL	4,460.00	189.760	391.781	28.592	359.288
Rb (μg/L)	0.03	15.76	0.805	1.410	0.098	1.727
Sr (μg/L)	4.30	19,600.00	1,710.361	2,681.413	44.061	4,352.000
Y (μg/L)	BDL	0.39	0.014	0.037	0.000	0.031
Zr (μg/L)	BDL	0.57	0.013	0.064	0.000	0.040
Nb (μg/L)	BDL	0.11	0.005	0.013	0.000	0.016
Mo (μg/L)	BDL	16.29	1.037	2.050	0.100	2.443
Ru (μg/L)	BDL	0.01	–	–	–	–
Pd (μg/L)	BDL	0.04	–	–	–	–
Ag (μg/L)	BDL	0.38	–	–	–	–
Cd (μg/L)	BDL	0.66	0.016	0.053	0.000	0.045
In (μg/L)	BDL	0.003	–	–	–	–
Sn (μg/L)	BDL	0.298	–	–	–	–
Sb (μg/L)	0.01	1.542	0.129	0.160	0.026	0.256
Te (μg/L)	BDL	0.30	0.027	0.048	0.000	0.073
I (μg/L)	BDL	95.19	13.532	16.505	1.274	31.486
Cs (μg/L)	BDL	19.25	0.106	1.115	0.000	0.020
Ba (μg/L)	0.29	589.21	93.296	121.874	3.784	286.157
La (μg/L)	BDL	0.59	0.005	0.036	0.000	0.006
Ce (μg/L)	BDL	1.39	0.008	0.081	0.000	0.009
Pr (μg/L)	BDL	0.14	0.000	0.009	0.000	0.001
Nd (μg/L)	BDL	0.52	0.002	0.034	0.000	0.009
Sm (μg/L)	BDL	0.10	0.000	0.008	0.000	0.003
Eu (μg/L)	BDL	0.05	0.001	0.004	0.000	0.006
Gd (μg/L)	BDL	0.08	0.000	0.007	0.000	0.004
Tb (μg/L)	BDL	0.01	–	–	–	–
Dy (μg/L)	BDL	0.06	0.001	0.006	0.000	0.002

Table 2 (Contd.)

	Min	Max	Mean	SD	10th P	90th P
Ho (μg/L)	BDL	0.01	–	–	–	–
Er (μg/L)	BDL	0.05	0.001	0.006	0.000	0.003
Tm (μg/L)	BDL	0.02	–	–	–	–
Yb (μg/L)	BDL	0.19	0.003	0.015	0.000	0.005
Lu (μg/L)	BDL	0.06	0.000	0.005	0.000	0.001
Hf (μg/L)	BDL	0.01	–	–	–	–
Ta (μg/L)	BDL	0.04	0.004	0.008	0.000	0.014
W (μg/L)	BDL	62.96	1.879	5.719	0.000	4.454
Re (μg/L)	BDL	0.27	0.008	0.025	0.000	0.016
Os (μg/L)	BDL	BDL	–	–	–	–
Pt (μg/L)	BDL	0.05	–	–	–	–
Au (μg/L)	BDL	0.76	0.003	0.043	0.000	0.005
Hg (μg/L)	BDL	1.12	–	–	–	–
Tl (μg/L)	BDL	0.23	–	–	–	–
Pb (μg/L)	BDL	2.94	–	–	–	–
Bi (μg/L)	BDL	0.05	–	–	–	–
Th (μg/L)	BDL	0.26	0.002	0.015	0.000	0.004
U (μg/L)	0.04	339.67	18.016	41.118	1.036	35.756

BDL below detection limits

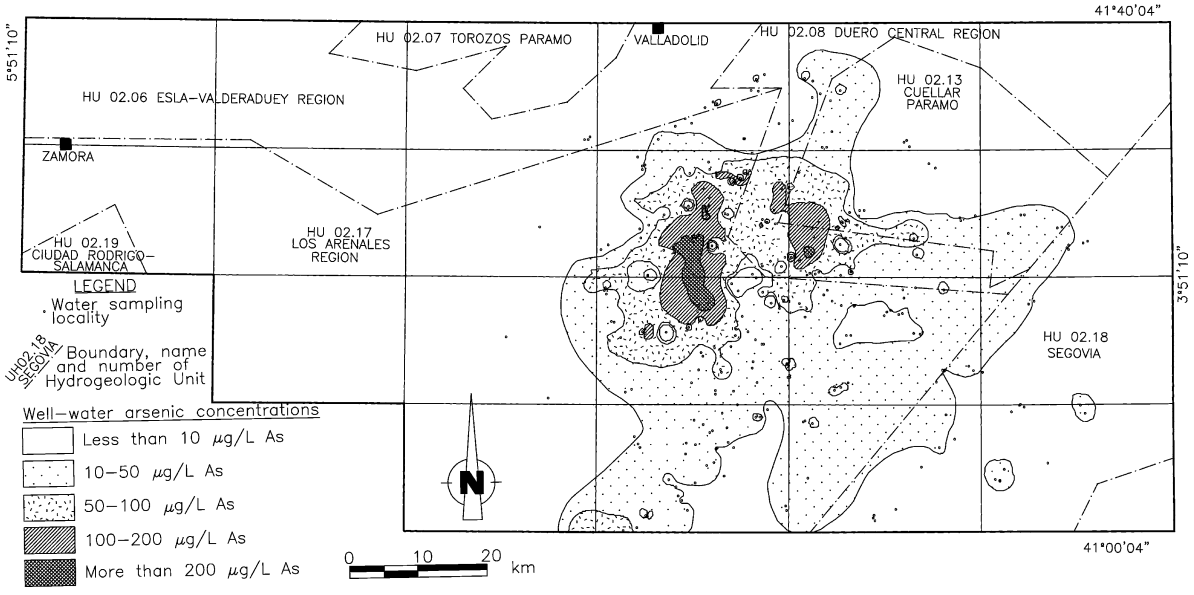

Fig. 4 Spatial distribution of the arsenic concentrations in groundwater. Data of the samples collected in September–October 2000

flow can be observed. All these data support the hypothesis that arsenic concentrations in groundwater are not derived from deep regional waters of high residence time.

The pH range obtained in groundwater sampling from the first survey is located between 5.9 and 10.6. pH poorly correlates with arsenic (0.44) but in general, as shown in Fig. 6, the highest arsenic values are related to pH values between 8 and 10.6. Arsenic shows a weak negative correlation (−0.29) with Eh values.

The correlation of arsenic concentration with carbonates, nitrates and sulphate concentrations is low (Table 3). There are zones with high nitrate concentration in the studied area, but detailed studies (Confederacion Hidrografica del Duero [CHD] 2001a, b, c, 2002a, b, 2003a, b, c) show that they do not coincide with the areas of maximum arsenic values. Although arsenic can be a component of some nitrate-bearing fertilizers and old pesticides (O'Neill 1995), the lack of correlation between arsenic and nitrates and the observed spatial distribution of arsenic (Fig. 4) suggests that the arsenic anomalies in groundwater in the studied area do not correspond to a model of pollution by dis-

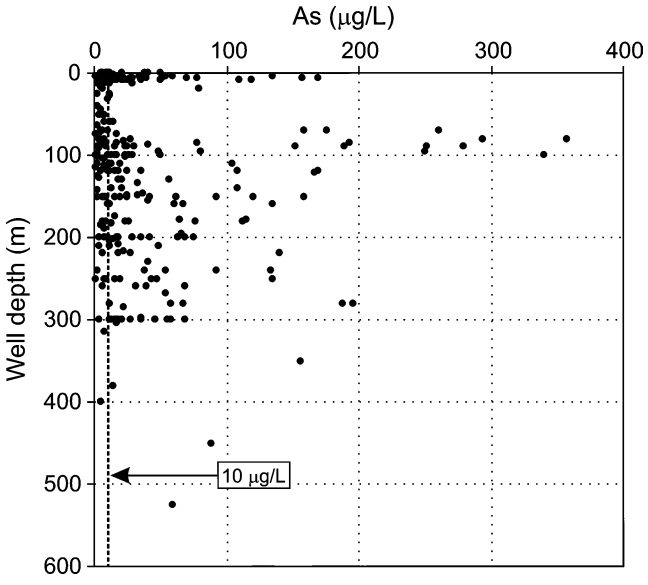

Fig. 5 Relationship between the arsenic concentrations in groundwater and the depth of the wells. Data of the samples collected in September–October 2000. Note that the maximum arsenic concentrations are recorded in wells about 70–100 m deep

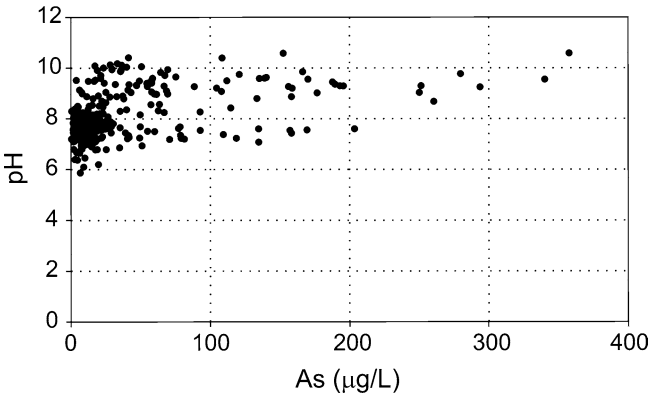

Fig. 6 Relationship between the arsenic concentrations and the pH in groundwater of the wells. Data of the samples collected in September–October 2000. Note that the highest arsenic values (above 205 μg/L) are related to pH values between 8.7 and 10.6

Table 3 Correlation matrix of arsenic and anions in groundwaters

	As	Cl^-	SO_4^{2-}	HCO_3^-	CO_3^{2-}	NO_3^-
As	1.00					
Cl^-	0.29	1.00				
SO_4^{2-}	0.07	0.27	1.00			
HCO_3^-	0.15	0.30	0.22	1.00		
CO_3^{2-}	0.40	0.29	−0.16	−0.11	1.00	
NO_3^-	−0.09	0.17	0.20	0.25	−0.25	1.00

Data of samples collected in September–October 2000

persion from a diffuse source located on the surface, associated with agricultural activities. However, abrupt arsenic variations have been detected in different sampling dates in some wells included in this study and in some wells of the network monitoring the nitrate concentration of the Duero Basin groundwater (CHD 2003a, b, c). These variations may be related to local and episodic anthropogenic arsenic pollution, possibly due to feedlot-raised poultry.

The correlation with other elements like nickel, strontium, copper and iron is also low, but a good correlation with vanadium and tungsten exists (Table 4). In fact, contouring of hydrochemical concentrations of these two elements in wells deeper than 20 m shows a very similar spatial distribution to that of arsenic. The total concentration of uranium in some samples exceeds 330 μg/L and its spatial distribution, for wells shallower than 20 m, is similar to that obtained from arsenic.

As shown in Fig. 7, the spatial distribution of arsenic concentrations analysed in the second sampling survey (April–May 2001) is similar to the one obtained in the first sampling survey (September–October 2000). The sites with concentrations higher than 150 μg/L arsenic recorded in the first survey showed smaller concentrations in the second survey. However, in the sites where arsenic concentrations in the first survey were lower than 150 μg/L, relevant decreases and increases were recorded. Significant (higher than 10 μg/L) variations between the two surveys are observed. For instance, in the second survey 38 wells showed lower arsenic concentrations, but 15 wells assayed higher ar-

Table 4 Arsenic correlation coefficients with trace elements in groundwaters

	Li	Mg	Al	Si	K	Ca	Sc	Ti	V	Cr	Mn	Fe	Ni	Cu
As	0.11	−0.05	−0.04	−0.06	−0.03	−0.11	−0.01	−0.08	*0.94*	0.53	−0.05	0.07	0.11	0.05
	Zn	Se	Br	Rb	Sr	Mo	Cd	Sb	Te	I	Ba	W	U	
As	−0.05	−0.06	0.01	−0.13	0.02	0.08	−0.06	0.10	−0.07	0.14	−0.22	*0.78*	0.09	

Samples collected in September–October 2000. Notice the good correlation with vanadium and tungsten

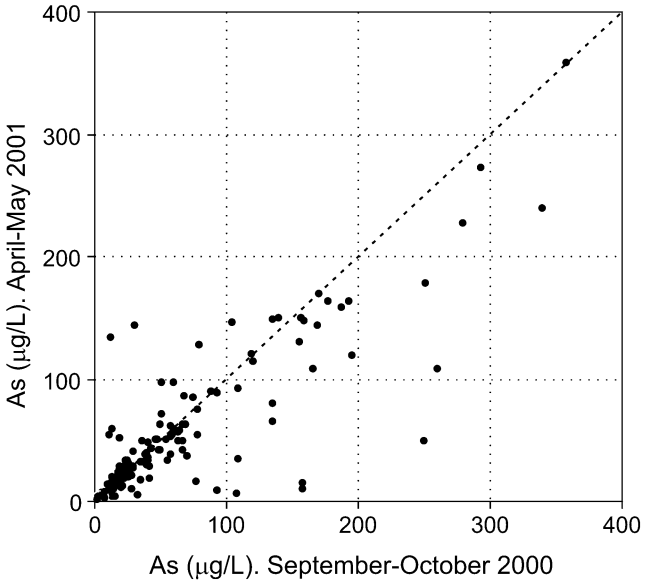

Fig. 7 Correlation between the arsenic concentrations in groundwater of the surveys carried out in September–October 2000 and April–May 2001. Note that there is a good correlation, except for the sites with concentrations higher than 150 μg/L arsenic recorded in the first survey, which showed smaller concentrations in the second survey

senic concentrations. The highest recorded absolute decrease occurred in the well that yielded the maximum arsenic values in both surveys, assaying from 613 μg/L (first survey) to 370 μg/L (second survey). The correlation of arsenic concentration with sulphate is low in the two surveys (0.07 and 0.23, in the first and second surveys, respectively), but in the second survey there is a higher correlation (0.90) in the waters with sulphate concentrations above 400 mg/L, which could be indicative of some participation of sulphide oxidation processes in the incorporation of arsenic to groundwater. This mechanism of arsenic mobilization also involves release of iron and decrease of pH (e.g. Schreiber et al.

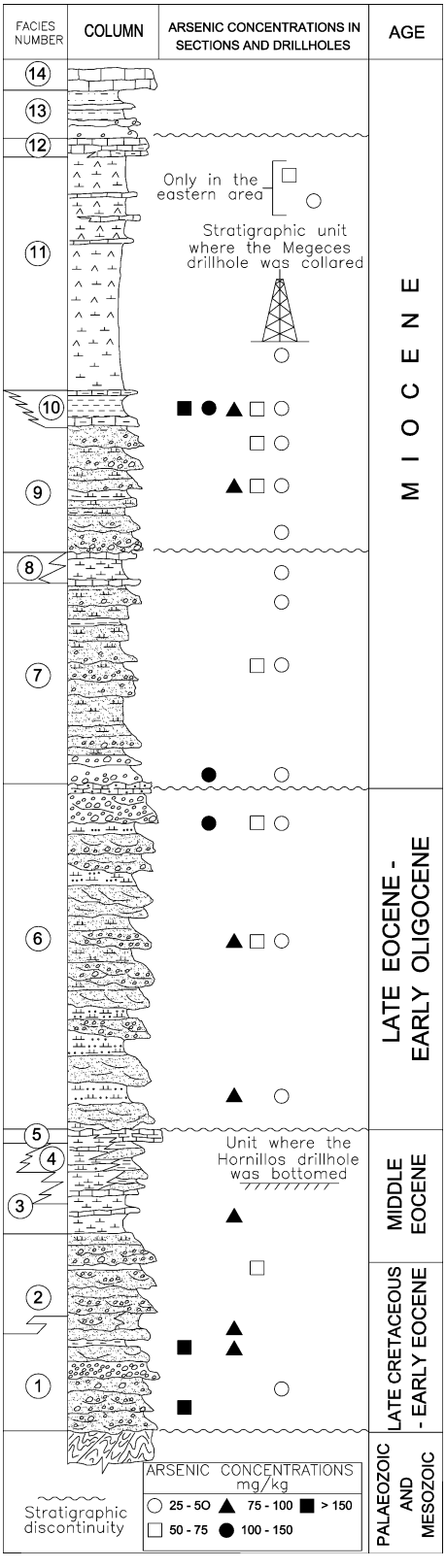

Fig. 8 Synthetic stratigraphic column valid for the studied area, showing the arsenic concentrations recorded in the samples of the 14 stratigraphic units and identified facies, as well as the main stratigraphic discontinuities. The column is schematic and the thickness of the different units is not to scale. *1* Zamora sandstone facies, *2* Zamora conglomerate facies, *3* Corrales Formation, *4* Tierra del Vino facies, *5* Santa Cecilia Formation, *6* Aldearrubia Formation (Toro facies, lower Olombrada and Valdefinjas Limestone), *7* Villaba de Adaja facies, *8* Dueñas facies, *9* Tierra de Campos facies, *10* Zaratan facies, *11* Cuestas facies, *12* lower Paramo facies, *13* intra-Paramos facies, *14* upper Paramo facies. Chronostratigraphic data after Armenteros et al. (2002) and Alonso-Gavilán et al. (2004)

Table 5 Summary of major and trace elements concentrations of the rock samples

	Min	Max	Mean	SD	10th P	90th P
n = 58						
SiO_2 (%)	15.15	84.10	52.458	14.135	33.144	69.164
Al_2O_3 (%)	2.34	20.86	13.613	4.962	6.468	19.354
$Fe_2O_{3(total)}$ (%)	1.07	39.92	7.509	6.377	3.422	12.806
MnO (%)	0.01	1.55	0.095	0.207	0.015	0.133
MgO (%)	0.03	14.99	3.361	3.090	0.473	5.752
CaO (%)	0.04	23.58	5.110	5.901	0.409	15.558
Na_2O (%)	0.02	1.54	0.432	0.321	0.130	0.829
K_2O (%)	0.11	5.09	3.141	1.284	1.275	4.522
TiO_2 (%)	0.11	0.93	0.582	0.220	0.258	0.843
P_2O_5 (%)	0.04	0.43	0.193	0.093	0.090	0.313
LOI (%)	2.34	37.22	12.864	7.189	5.762	22.814
Total (%)	90.83	100.37	99.354	1.357	98.821	100.195
n = 553						
As (mg/kg)	BDL	337.00	23.050	28.965	3.900	48.320
Ag (mg/kg)	BDL	BDL	–	–	–	–
Au (mg/kg)	BDL	BDL	–	–	–	–
Ba (mg/kg)	BDL	3,900.00	455.157	279.222	200.000	690.000
Br (mg/kg)	BDL	36.70	1.184	3.556	0.000	4.300
Ca (mg/kg)	BDL	47.00	6.570	9.800	0.000	19.000
Co (mg/kg)	BDL	48.00	8.602	6.619	2.000	16.000
Cr (mg/kg)	BDL	132.00	39.382	23.786	14.000	72.000
Cs (mg/kg)	BDL	21.00	6.653	4.158	2.000	13.000
Fe (mg/kg)	0.040	27.10	2.508	2.174	0.724	4.688
Hf (mg/kg)	BDL	24.00	3.336	2.437	1.000	6.000
Hg (mg/kg)	BDL	BDL	–	–	–	–
Ir (mg/kg)	BDL	BDL	–	–	–	–
Mo (mg/kg)	BDL	123.00	3.425	8.784	0.000	10.000
Na (mg/kg)	BDL	1.920	0.441	0.400	0.070	1.020
Ni (mg/kg)	BDL	136.00	–	–	–	–
Rb (mg/kg)	BDL	277.00	106.090	55.596	40.200	176.000
Sb (mg/kg)	BDL	11.30	1.351	1.188	0.300	2.600
Sc (mg/kg)	BDL	20.00	7.298	4.591	2.200	14.280
Se (mg/kg)	BDL	6.00	–	–	–	–
Sn (mg/kg)	BDL	0.10	–	–	–	–
Sr (mg/kg)	BDL	0.80	–	–	–	–
Ta (mg/kg)	BDL	3.20	0.252	1.006	0.000	1.800
Th (mg/kg)	BDL	27.60	9.682	4.975	3.600	16.300
U (mg/kg)	BDL	216.00	5.019	12.832	1.200	8.580
W (mg/kg)	BDL	321.00	4.320	25.824	0.000	6.000
Zn (mg/kg)	BDL	276.00	29.839	79.345	0.000	130.000
La (mg/kg)	BDL	75.80	27.194	12.674	11.200	44.400
Ce (mg/kg)	BDL	223.00	57.221	27.715	22.000	93.800
Nd (mg/kg)	BDL	139.00	21.297	12.313	8.200	35.000
Sm (mg/kg)	BDL	19.20	4.776	2.303	1.900	7.800
Eu (mg/kg)	BDL	3.10	0.932	0.455	0.400	1.500
Tb (mg/kg)	BDL	1.60	–	–	–	–
Yb (mg/kg)	BDL	5.50	1.999	1.032	0.700	3.300
Lu (mg/kg)	BDL	0.81	0.304	0.159	0.102	0.510

BDL below detection limits

2003). Given the pH values (> 7) and the low correlation observed between arsenic and iron in those samples with high sulphate concentrations, the oxidative dissolution of sulphides as pyrite cannot be considered as the main mechanism responsible for the presence of arsenic in the groundwater, even if some participation could take place. On the other side, the low arsenic–iron correlation precludes the reductive dissolution of arsenic-rich oxides and hydroxides as the responsible mechanism for arsenic mobilization. Thus, the recorded hydrochemical pattern suggests other mechanisms, such as desorption from iron and manganese oxides, related to an alkaline and oxidizing environment, as indicated by Smedley and Kinninburgh (2002, p. 553).

Geology and geochemistry of the sedimentary facies

The stratigraphic, sedimentological and palaeogeographical aspects of the Cenozoic sediments that fill up the Duero Basin have been studied in numerous works, which have been summarized by Armenteros et al. (2002) and Alonso-Gavilán et al. (2004).

The study of the 69 stratigraphic sections and the 7 core holes allowed reconstruction of the regional stratigraphic column shown in Fig. 8 and the collection of 553 rock samples representative of the different lithologies constituting the stratigraphic units. Samples with concentrations above the arsenic geochemical background (28.50 mg/kg) have been recorded in all the stratigraphic units. Thus, anomalous concentrations are not restricted to certain formations, lithologies or sedimentary or lithostratigraphic units, although some units show notably higher arsenic concentrations than the others (Fig. 8).

The results of the geochemical analysis of the 553 rock samples, summarized in Table 5, show a strong asymmetric distribution of frequencies, as displayed in Fig. 9, with peak values up to 337 mg/kg arsenic. The background value calculated following the modified Lepeltier method proposed by Matschullat et al. (2000) is 28.5 mg/kg arsenic. This value is similar to those mentioned in the literature for lutitic sedimentary formations, like the value of 28.40 mg/kg arsenic of the North American Shales Composite (NASC) of Gromet et al. (1984). A total of 131 samples (23.6%) showed anomalous arsenic concentration above the background value.

Considering the 553 collected samples, a moderate to high correlation of arsenic with iron and a moderate correlation with antimony are observed (Table 6). In the 131 anomalous samples set there is a moderate correlation with iron, but correlation with antimony decreases (Table 6). Except for the arsenic associated with iron minerals, which seems to be dominant, the inconsistent results of the correlation study of trace elements show that arsenic has to necessarily be related to different forms of occurrence in the sedimentary rocks.

In the 58 selected samples containing more than 43.5 mg/kg arsenic, the concentrations of major elements (oxides) show some correlation (0.57) with the concentrations of $Fe_2O_{3(total)}$ as expected, being negative or very low for the other oxides, including MnO (Table 7).

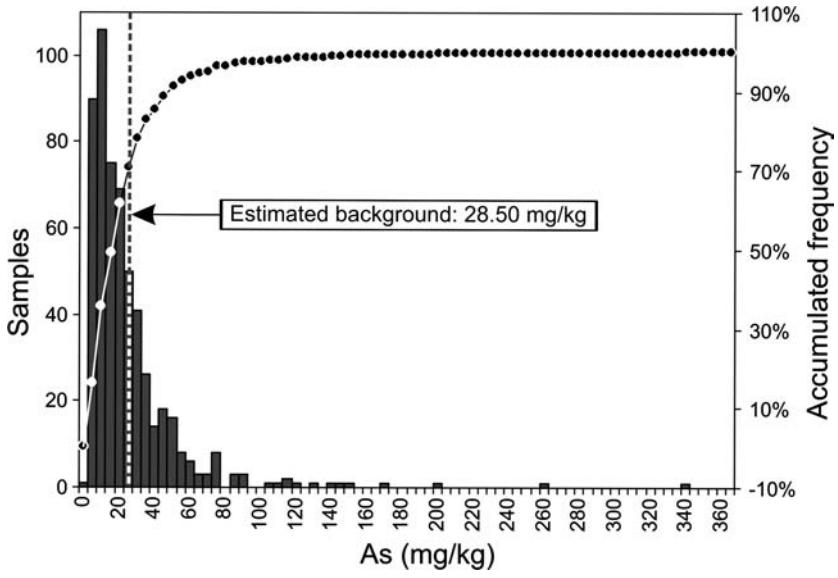

Fig. 9 Frequency distribution of the arsenic concentrations of the 553 rock samples. The position of the geochemical background is pointed out

Fourteen stratigraphic units have been distinguished in the area. They have been grouped into five stratigraphic intervals, shown in Fig. 10, some of which are bounded by stratigraphic discontinuities that partly coincide with that previously recognized by several authors in a wider area (Portero et al. 1982; Corrochano and Armenteros 1989; Armenteros and Corrochano 1994; Pérez González et al. 1994; Santisteban and Martín-Serrano 1991; Santisteban et al. 1996a, b; Armenteros et al. 2002; Alonso-Gavilán et al. 2004). The sediments included in these stratigraphic intervals show a marked spatial continuity in the studied sector of the basin and have helped to describe the spatial distribution of the arsenic concentration in the rocks.

These intervals are, from bottom to top (Fig. 10): Late Cretaceous–Middle Eocene interval, Late Eocene–Early Oligocene interval, Late Oligocene–Middle Miocene interval, Middle Miocene interval (Zaratan facies) and Middle–Late Miocene interval (Cuestas–Paramos facies).

The rocks belonging to the Late Cretaceous (Pol et al. 1992), to the Palaeocene, to the Eocene and to part of the Oligocene, crop out in the western, southern and southeastern sectors of the studied area (Fig. 1b). At least part of the Palaeocene and part of the Late Oligocene sediments seem to be absent in a large part of the basin (Fig. 10, Armenteros et al. 2002; Alonso-Gavilán et al. 2004), and the Neogene sediments crop out in the

Table 6 Correlation coefficients between the arsenic concentrations and other trace elements analysed in the 553 samples of sedimentary rocks and the subpopulation of 131 samples with arsenic concentration higher than 28,50 mg/kg

	Ba	Br	Co	Cr	Cs	Fe	Hf	Mo	Na	Ni	Rb	Sb	Sc	Sn
As (553 samples)	0.17	−0.03	0.32	0.37	0.26	*0.69*	0.08	0.26	−0.12	0.09	0.17	*0.55*	0.39	−0.09
As (samples with As > 28.50 mg/kg)	0.05	−0.03	0.06	0.03	−0.12	*0.60*	−0.11	0.31	−0.17	0.02	−0.14	*0.39*	0.00	−0.06
	Sr	Ta	Th	U	W	Zn	La	Ce	Nd	Sm	Eu	Tb	Yb	Lu
As (553 samples)	0.12	0.23	0.34	0.11	0.01	0.25	0.3	0.29	0.21	0.29	0.27	0.19	0.28	0.28
As (samples with As > 28.50 mg/kg)	−0.06	0.11	0.03	0.13	0.08	−0.06	−0.16	0.01	−0.01	−0.13	−0.06	−0.12	0.01	−0.02

Notice the correlation with iron and antimony

Table 7 Correlation coefficients of arsenic concentrations and major elements (58 samples)

	SiO_2	Al_2O_3	$Fe_2O_{3(total)}$	MnO	MgO	CaO	Na_2O	K_2O	TiO_2	P_2O_5	LOI
As	−0.06	−0.39	*0.57*	0.05	−0.24	−0.04	−0.17	−0.24	−0.32	0.05	0.09

LOI loss in ignition

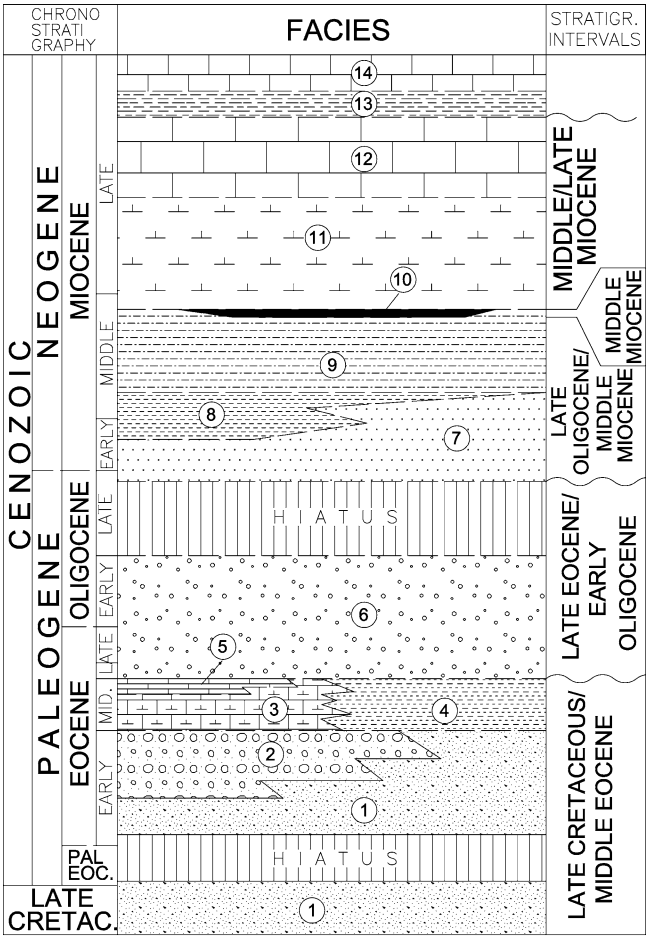

Fig. 10 Stratigraphic intervals differentiated to analyse the arsenic distribution in the rocks inside the studied area. Numbers of the units and facies that constitute each interval coincide with those expressed in Fig. 8

central and northern part (Armenteros 1986; Fig. 1b). Stratigraphic intervals 1–4 are the main constituents of the hydrogeological units mentioned in Geological and hydrogeological setting, except for the Middle–Late Miocene interval (Cuestas–Paramos facies), which constitutes most of the Torozo Paramo and Cuellar Paramo Hydrogeological Units.

Arsenic concentration in the rocks of the Late Cretaceous–Middle Eocene interval

The rocks of this interval that lie unconformably on the Variscan basement (Jiménez 1973; Corrochano 1977; Alonso Gavilán 1981; Jiménez et al. 1983) crop out in the western part of the studied area (Fig. 1). The interval consists of sandstones and conglomerates with sandy matrix and ferruginous cement, grading into lutites, marls and limestones in the upper part (Alonso Gavilán 1984, 1986; Figs. 9, 10). This unit contains ferricretes, more abundant towards the lower part, as well as silcretes (Corrochano 1982; Fernández García et al. 1989). Among the 35 rock samples analysed in this interval, 7 samples with high arsenic concentration up to 258 mg/kg have been identified. Abnormally high arsenic values, delineating the anomaly in the northwestern area depicted in Fig. 11, occur in samples that generally correspond to rocks of the lower part of the interval, containing iron oxides and hydroxides, mainly hematite and goethite, associated with ferricretes or with ferruginous cements and iron fragments in the sandstones.

Arsenic in the rocks of this interval shows a marked correlation with iron and antimony, although it seems to be heterogenously distributed in the iron oxides and hydroxides, even at a microscopic scale. The iron minerals have possibly been formed during the early cementation stages, developed under a relatively warm and humid climate (Armenteros et al. 2002). These conditions are also indicated by the presence of kaolinite (Bustillo and Martín-Serrano 1980; Molina et al. 1997), which sometimes appears as essential mineral, reflecting an important water circulation in the vadose area. Due to cementation, pore-space volume and pore interconnection are low, and consequently solid phase–water interaction is restricted. Evidence of mineral instability, as reaction or dissolution textures, has not been observed. The rocks of this interval constitute a potential source of arsenic that could pass to the groundwater. Nevertheless, correlation between arsenic concentration in these rocks and in groundwater has not been established yet, as only the Hornillos drill hole (Fig. 2) intersects the rocks of the upper part of this interval (Fig. 9), but the rocks of its lower part, which show some of the highest values in arsenic, were not drilled in this hole.

Arsenic concentration in the rocks of the Late Eocene–Early Oligocene interval

This interval, composed of conglomerates, gravels, sands and silts (Figs. 9, 10), crops out in the western and eastern areas, being recognized by core drilling in the central area. From a total of 120 analysed rock samples, 34 samples contain arsenic concentrations above background values, with peak concentrations up to 127 mg/kg arsenic. The rocks of the Late Eocene–Early Oligocene interval show, in general, low arsenic values (below the regional background), except in the northwestern area, as shown in Fig. 12, where remarkable anomalies have been recorded. In the central sector, anomalies are weaker, but they coincide with the area of main arsenic anomalies in groundwater (Fig. 4).

The arsenic concentrations in the samples of this group show a distinct correlation with antimony and

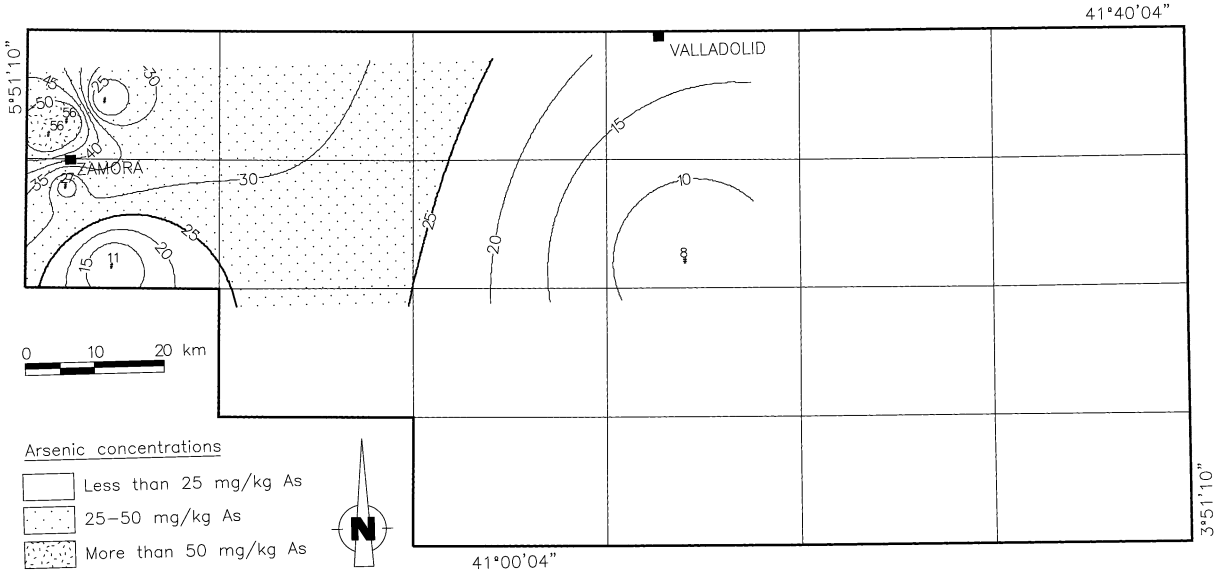

Fig. 11 Spatial distribution of the mean arsenic values of the samples corresponding to the Late Cretaceous–Middle Eocene interval. In the northwestern part, where this unit crops out, a lithogeochemical anomaly with a mean value of 60 mg/kg arsenic has been detected. The value of the central area corresponds to the Hornillos drill hole, which has only intersected the rocks of the upper part of the interval

moderate to high with iron. The arsenic occurrence seems to be linked to iron oxides and hydroxides, although no grains of those minerals with detectable arsenic concentrations have been identified. Part of the iron oxides can be derived from the oxidation of pyrite, as indicated by the occurrence of jarosite. In samples where arsenic does not correlate with iron, the mineralogical observations carried out with SEM-EDX confirm that the arsenic is associated with manganese oxides.

Fig. 12 Spatial distribution of the mean values of arsenic of the samples corresponding to the Late Eocene–Early Oligocene interval. In the northwestern part, a lithogeochemical anomaly with maximum mean values of 58 mg/kg arsenic and two weak anomalies in the central part are recognized

Arsenic concentration in the rocks of the Late Oligocene–Middle Miocene interval

The Late Oligocene–Middle Miocene interval is constituted by arkoses, sands and lutites, which grade into carbonate sediments as well as sandy conglomerates toward the central part of the studied area (Figs. 9, 10). Out of the 235 collected samples, 32 show arsenic con-

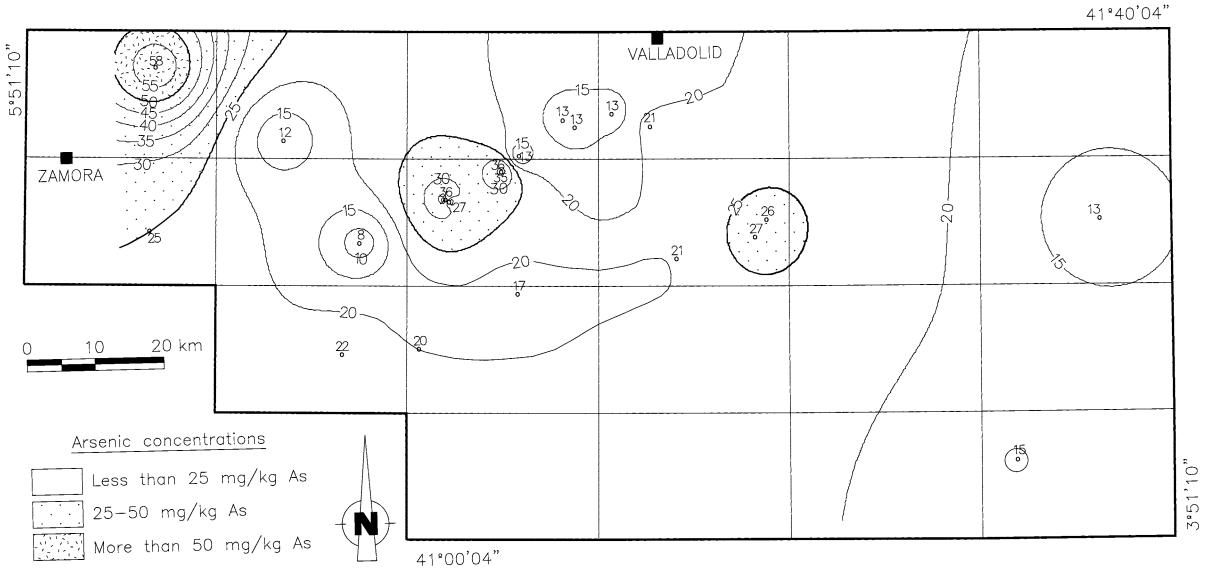

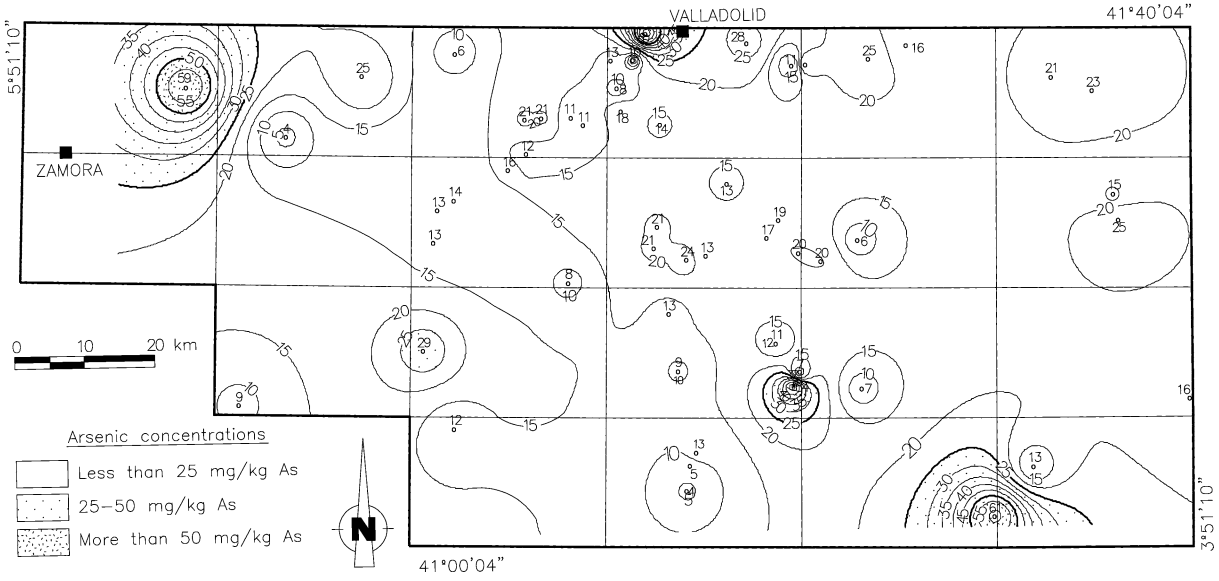

Fig. 13 Spatial distribution of the mean arsenic values of the samples corresponding to the Late Oligocene–Middle Miocene interval. Several lithogeochemical anomalies, with mean values of up to 68 mg/kg arsenic, are recognized

centrations above the background value, reaching a maximum value of 109 mg/kg. However, the arsenic values are generally low, except for local significant anomalies illustrated in Fig. 13. The arsenic anomaly recorded in the northwestern area, which correlates with those anomalies recorded in previous intervals, corresponds to samples of the lower portion of this stratigraphic interval. The anomalies recorded in the central and southeastern areas show a positive correlation with the arsenic anomalies detected in groundwater (Fig. 4). The maximum arsenic values and the highest number of anomalous samples correspond to samples collected in the transition between the rocks of this interval and the rocks of the following Middle Miocene interval (Zaratan facies), located above.

Arsenic shows certain (0.73) correlation with Mn, illustrating an occurrence related to Mn minerals as oxides, and a moderate to low correlation with iron. In some samples, the arsenic and iron geochemical patterns suggest that partial desorption of arsenic from iron oxides is the feasible mechanism for releasing arsenic to groundwater. This mechanism only involves arsenic mobilization from the solid phase, contrary to the release by mineral dissolution which involves both mobilization of iron and arsenic, as shown in Fig. 14a, b. Thus, the observed pattern could be related to Fe samples originally rich in arsenic, which was released later. Other forms of arsenic occurrence have also been identified by SEM-EDX in apparently authigenic microaggregates of illite-type clays and associated with Ti–Fe oxides, as observed in Fig. 15, detrital grains of Ti–Fe–Mn oxides and detrital phyllosilicates of moscovitic–illitic composition. Thus, arsenic accumulation took place by sedimentary deposition of arsenic-rich detrital minerals and coprecipitation and absorption in authigenic phyllosilicates and oxides. Adsorption implies immobilization of arsenic in the solution for electrostatic attraction onto the surface of the oxides and phyllosilicates. Adsorbed arsenic may be released by desorption and ion exchange mechanisms if certain conditions like pH increase or high concentration of competitive ionic species occur (e.g. Welch et al. 2000; Smedley and Kinninburgh 2002).

Arsenic concentration in the rocks of the Middle Miocene interval, Zaratan facies

The Zaratan facies, Middle Miocene in age, is constituted by marls and clays with organic matter deposited in a palustrine environment (Carballeira and Pol 1986; Corrochano et al. 1986; Corrochano and Armenteros 1989; Armenteros et al. 2002). This facies is mainly considered as an aquitard and crops out in the central sector of the studied area, grading both toward east and west to coarser-grained sediments (Figs. 9, 10). From the 78 rock samples collected in this unit, 42 show arsenic concentrations above background, including the maximum values recorded in this study (337 mg/kg arsenic), representing the highest number of anomalies and the highest arsenic concentrations recorded in the study area. An adjusted correspondence among the spatial distribution of the strongly anomalous values of the arsenic concentration in this unit, shown in Fig. 16, and those recorded in the groundwater (Fig. 4) is remarkable. As can be observed, all the arsenic anomalous values detected in groundwater are included in the wide

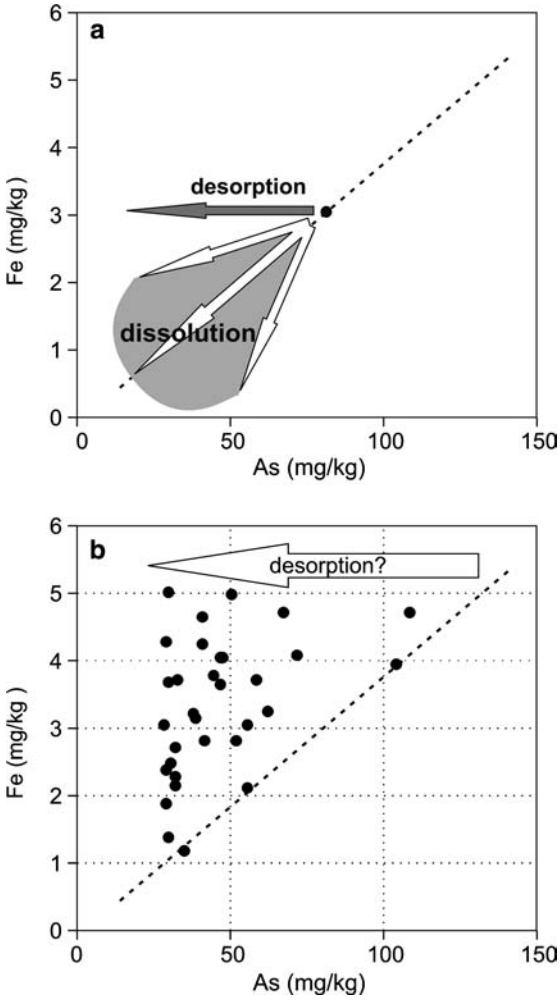

Fig. 14 **a** Theoretical model for the variations of iron and arsenic in the solid phase, for the proposed mechanisms of the arsenic release from iron oxides. If the dissolution processes were dominant, the results of the analysis of both elements would be concentrated in the *grey* area. Alternatively, if the dominant process were desorption, the geochemical relation between both elements would be concentrated above the *dashed line*. **b** Distribution of arsenic and iron concentration of the rock samples of the Late Oligocene–Middle Miocene interval, with arsenic concentration above 28.50 mg/kg arsenic. As can be observed, the cluster of the arsenic and iron relationship suggests that desorption was the dominant mechanism for the release of arsenic into groundwater

area of lithogeochemical anomalies of this unit. The arsenic concentration in both groundwater and rocks of the Zaratan facies decreases from the maximum reached values in the central–eastern area toward the east and west, as the palustrine organic-rich facies grade into more proximal coarser-grained alluvial facies. Arsenic appears to be mainly associated with the presence of the organic matter contained in the lutites and with iron oxides, which are more abundant in the central sector, and gradually decreases toward the margins of the basin as the concentration in sands and silts increases.

The correlation of the arsenic concentration is moderate (0.64) with molybdenum and weak (0.47) with iron. The geochemical pattern is different if compared to the other considered stratigraphic intervals. The occurrence of high concentrations of arsenic is associated with high iron concentrations and a higher concentration of organic carbon. The analytical results of the organic carbon concentration from 17 samples collected in the Zaratan facies, shown in Fig. 17, allow for the differentiation of three populations with regard to arsenic: a group of samples with low organic carbon concentration (0.05–0.08%) and high concentrations in arsenic; a group of samples (0.13–1.05% carbon) that show some correlation between the values of organic carbon and arsenic and a third group with relatively high concentrations of carbon (0.78–0.81%) and arsenic concentrations near the background value. These relationships, between arsenic, iron and organic carbon, suggest the existence of coprecipitation processes of arsenic with pyrite in reducing organic matter-rich environment, and later oxidation–dissolution of the sulphide in oxidizing environment. Alternatively, samples with some correlation between organic carbon and arsenic may be representative of arsenic sorption onto organic matter and authigenic iron oxides. And finally, samples with high content of iron and organic carbon, but low values of arsenic, may be representative of subsequent arsenic desorption from the organic matter and iron oxides.

From a mineralogical point of view, the presence of arsenic in the Zaratan facies is related to authigenic pyrite, as observed in Fig. 18, iron oxides generated from the oxidation of the authigenic pyrite and organomineral compounds related to the organic matter. The markedly reducing palustrine depositional environments of this unit were favourable for the bacterial activity that caused coprecipitation of arsenic in the pyrite and its adsorption in the organic carbon. Later on, as a consequence of a redox change in the sediment, jarosite and iron oxides were generated from the oxidation of the pyrite. At that stage, the released arsenic could be newly trapped by coprecipitation and adsorption processes related to the iron oxides and organic matter. Note that organic matter has a very high capacity of adsorption of anionic species in acidic environments as those generated during pyrite oxidation. Afterwards, arsenic could be mobilized from both iron oxides and organic matter by desorption in an alkaline environment (e.g. Welch et al. 2000; Smedley and Kinninburgh 2002; Gurung et al. 2005).

Arsenic concentration in the rocks of the Middle–Late Miocene interval, Cuestas and Paramos facies

The Cuestas facies are constituted by a succession of clays, marls and gypsum, the hydrogeological behav-

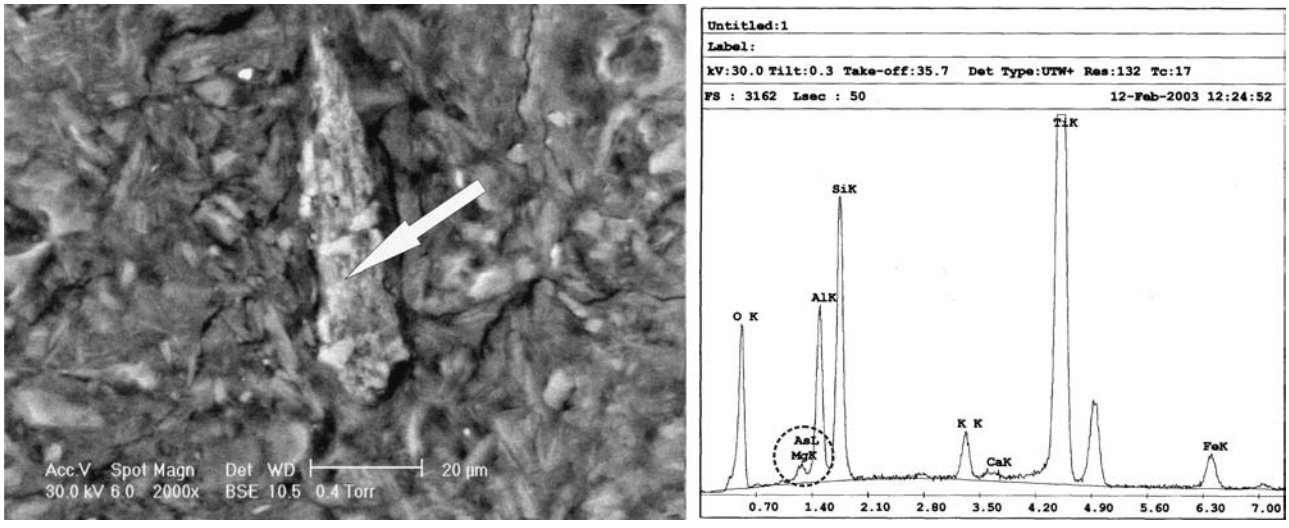

Fig. 15 Backscattered electron (BSE) image and energy dispersive X-ray (EDX) spectrum of an authigenic micro-aggregate formed by phyllosilicates, and titanium and iron oxides in a sample (powder) of the Late Oligocene–Middle Mioceno interval. The *arrow* in the picture points out the micro-analysis spot. The *circle* stands out the sector of the spectrum where a pattern that can be attributed to arsenic appears

iour of which is mainly considered as that of an aquitard separating the multilayered aquifer composed of the previous units from the uppermost aquifer, constituted by the Paramos facies. The Paramos facies is composed of two limestone units, the lower and upper Paramo units, deposited in lacustrine environments (Carballeira and Pol 1986; Corrochano et al. 1986; Armenteros 1991; Armenteros et al. 1995; Mediavilla et al. 1996), separated by an ''intra-Paramo'' facies composed of siliciclastic sediments (Figs. 9, 10), which crop out in the central and eastern parts of the studied area. The Paramos facies constitute a free aquifer represented in the Torozo Paramo and Cuellar Paramo Hydrogeological Units (Fig. 2). Only 16 of the 85 analysed rock samples from the Cuestas facies have arsenic concentrations higher than the background value. One sample reached 139 mg/kg arsenic, and the rest do not overcome the 61.6 mg/kg arsenic. Concentrations in arsenic are generally low, recording the four areas of small anomalies shown in Fig. 19. Analytical

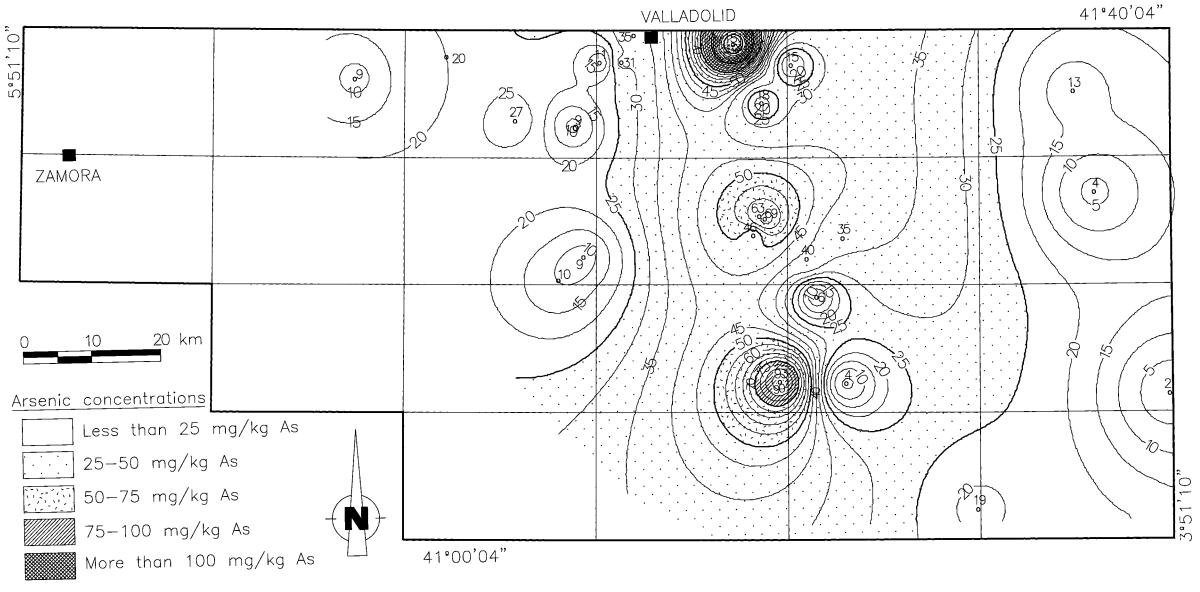

Fig. 16 Spatial distribution of the mean arsenic values of the samples corresponding to the Zaratan facies (Middle Miocene interval). The extensive lithogeochemical anomalies are concentrated in the central area reaching mean values of up to 151 mg/kg arsenic

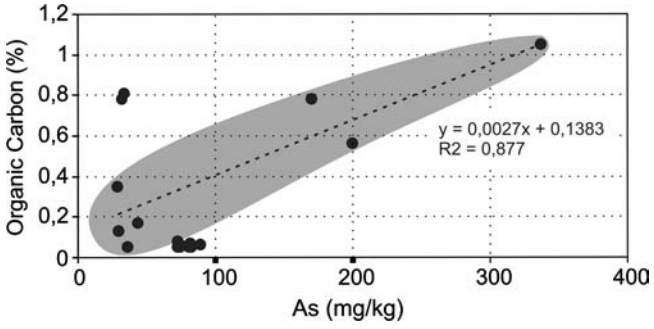

Fig. 17 Correlation between the arsenic concentrations and organic carbon in the Zaratan facies. Note that there is a subpopulation of samples (*shaded area*) that shows a good correlation (0.877). The equation of the regression line of the points is included for reference

results suggest that, except for some local areas, the rocks of this interval are not a significant source for arsenic present in the groundwater of the region. The arsenic concentrations in the rocks of this interval show a moderate to low correlation with iron. The geochemical pattern of the arsenic and iron relationship is interpreted as evidence of arsenic desorption processes from originally arsenic-rich iron minerals. The presence of arsenic has been recognized in grains of iron oxides and inherited titanium.

Discussion and conclusions

Abnormally high arsenic concentrations in poisonous amounts that make the groundwater of the southeastern part of the Duero Basin inadequate for human consumption have been measured. Arsenic is naturally occurring and is related to the high arsenic concentrations in the sediments constituting the system of aquifers and aquitards conformed by the Cenozoic sediments filling up the basin. However, the possibility of some local and occasional polluting contributions of anthropogenic origin cannot be discarded.

In all the studied sedimentary units, rock samples with arsenic concentrations greater than the geochemical background were found, but facies, arsenic concentrations and mineralogical forms are different. A remarkable degree of correlation between the main arsenic anomaly in groundwater and the large lithogeochemical arsenic anomaly related to the Middle Miocene Zaratan facies has been observed. This correlation indicates that the organic-rich sediments of this unit constituted the main source of arsenic for the recorded arsenic anomaly in groundwater.

Lithogeochemical anomalies contributing to the release of arsenic to groundwater also include the transition between the sediments of the Middle Miocene Zaratan facies and the rocks of the Late Oligocene–Middle Miocene interval. The rocks of the Late Cretaceous–Middle Eocene, Late Eocene–Early Oligocene and Late Oligocene–Middle Miocene intervals constitute a potential arsenic source that could pass into the groundwater of the northwestern area and to the deep aquifers of the central sector of the studied area.

The identified arsenic occurrence in the studied sedimentary rocks is linked to iron oxides and hydroxides, manganese oxides, authigenic pyrite, inherited titanium–iron oxides (detrital grains), phyllosilicates (authigenic

Fig. 18 Backscattered electron (BSE) image and energy dispersive X-ray (EDX) spectrum of a grain of authigenic pyrite in a sample (powder) of the Zaratan facies. The *arrow* in the picture points out the micro-analysis spot. The relatively high silica and aluminium picks are due to the "noise" caused by small badges of clays fixed to the grain. The *circle* stands out the area of the spectrum where a pattern attributable to arsenic appears

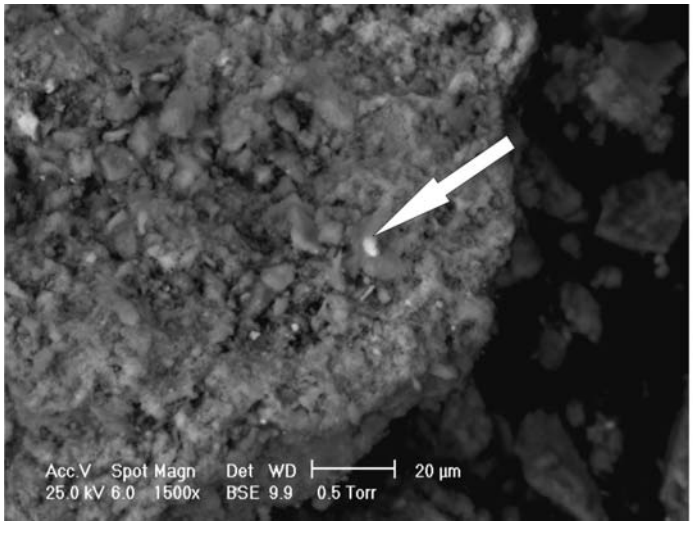

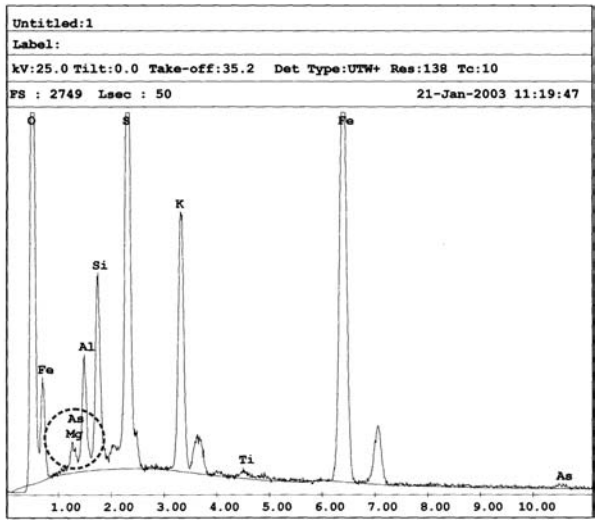

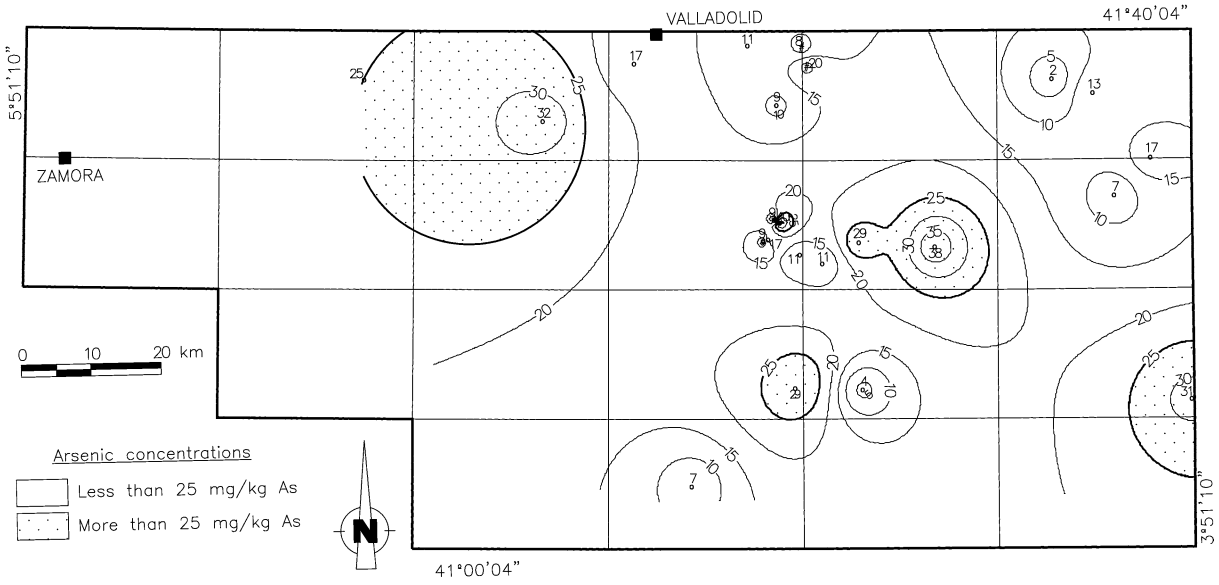

Fig. 19 Spatial distribution of the mean arsenic values of the samples corresponding to the Cuestas and Paramos facies (Middle–Late Miocene interval). Four weak lithogeochemical anomalies with mean values of up to 38 mg/kg arsenic are recognized

illite and inherited detrital grains of white mica) and organomineral compounds related to the organic matter. The initial accumulation in the case of the authigenic pyrite and of the organomineral compounds of the Zaratan facies is due to coprecipitation in the pyrite and adsorption in the organic compounds, in a reducing environment related to the palustrine sedimentary environment on which this facies was developed. In contrast, the arsenic-rich iron oxides and hydroxides are concentrated in ferricretes, generated under oxidizing environments. One example is the arsenic associated with the palaeosoils found in the siliciclastics of the Late Cretaceous–Middle Eocene interval.

In the rocks considered in this study, the fundamental mechanism of arsenic mobilization to groundwater corresponds to the arsenic desorption in iron and manganese oxides and hydroxides in oxidizing and alkaline conditions. Besides mobilization starting from oxides and hydroxides, certain mobilization also took place, especially in connection with mechanisms of arsenic desorption from the organic matter and oxidation–dissolution of the pyrite in the organic-rich sediments of the Zaratan facies.

Results obtained in this study regarding the spatial correlation between the arsenic anomalies in groundwater and in rocks allow the planning of further works in other areas with high arsenic concentrations in groundwater, highlighting those on which the lithologies and deposition environments can be appropriate to fix arsenic, and its later mobilization to the groundwater. However, due to the anisotropy and heterogeneity of the aquifers and aquitards and the action of bacterial populations, among other factors, further research is needed to explain the diversity of arsenic concentrations observed in some wells.

Acknowledgements The authors thank the Direccion General de Obras Hidraulicas y Calidad de las Aguas of the Ministerio de Medio Ambiente, the Confederacion Hidrografica del Duero, the authorization for the publication of the studies carried out by the authors and synthesized in this work. We wish to thank the editor Dr. Jan Schwarz Bauer and an anonymous referee who provided useful criticism and valuable suggestions for the improvement of the manuscript. Our gratitude to José L. Barroso (Confederacion Hidrografica del the Duero), for the contribution of some of the hydrochemical data used in this publication, and to Antonio Hernández and Pedro del Olmo for their valuable participation in this study. The work presented here was partially funded by the project GR/AMB/0934/2004 (Comunidad de Madrid).

References

Alonso Gavilán G (1981) Estratigrafía y sedimentología del Paleógeno en el borde suroccidental de la Cuenca del Duero (provincia de Salamanca). PhD, University of Salamanca

Alonso Gavilán G (1984) Evolución del sistema fluvial de la Formación Areniscas de Aldearrubia (Paleógeno superior) (Provincia de Salamanca). Mediterránea 3:107–130

Alonso Gavilán G (1986) Paleogeografía del Eoceno superior-Oligoceno en el SO de la Cuenca del Duero (España). Stvdia Geol Salmant 22:71–92

Alonso-Gavilán G, Armenteros J, Carballeira A, Corrochano A, Huerta P, Rodríguez JM (2004) Cuenca del Duero. In: Vera JA (ed) Geología de España. SEG-IGME, Madrid, pp 550–556

Aragonés Sanz N, Palacios Díez M, Avello de Miguel A, Gómez Rodríguez P, Martínez Cortés M, Rodríguez Bernabeu MJ (2001) Nivel de arsénico en abastecimientos de agua de consumo de origen subterráneo en la Comunidad de Madrid. Rev Esp Salud Publica 75:421–432

Armenteros I (1986) Estratigrafía y sedimentología del Neógeno del sector suroriental de la Depresión del Duero. Ed. Diputación de Salamanca. Serie Castilla y León, pp 1–471

Armenteros I (1991) Contribución al conocimiento del Mioceno lacustre de la Cuenca terciaria del Duero (sector centro-oriental, Valladolid-Peñafiel-Sacramenia-Cuéllar). Acta Geol Hisp 26:97–131

Armenteros I, Corrochano A (1994) Lacustrine record in the continental Tertiary Duero basin (northern Spain). In: Gierlowski E, Kelts K (eds) Global geological record of Lacustrine Basins. Cambridge University Press, Cambridge, pp 47–52

Armenteros I, Bustillo MA, Blanco JA (1995) Pedogenic and groundwater processes in closed Miocene basin (northern Spain). Sediment Geol 99:17–36

Armenteros I, Corrochano A, Alonso-Gavilán G, Carballeira J, Rodríguez JM (2002) Duero basin (northern Spain). In: Gibbons W, Moreno T (eds) The geology of Spain. 13 tertiary. The Geological Society of London, London, pp 309–315

Barroso JL, Lillo J, Sahún B, Tenajas J (2002) Caracterización del contenido de arsénico en las aguas subterráneas de la zona comprendida entre el río Duero, el río Cega y el Sistema Central. Presente y Futuro del agua subterránea en España y la Directiva Marco Europea, Zaragoza, pp 77–84

Bustillo MA, Martín-Serrano A (1980) Caracterización y significado de las rocas silíceas y ferruginosas del Paleoceno de Zamora. Tecniterrae 36:14–29

Calvo Revuelta C, Álvarez-Benedí J, Andrade Benítez P, Marinero Díez P, Bolado Rodríguez S (2003) Contaminación por arsénico en aguas subterráneas en la provincia de Valladolid: variaciones estacionales. Estudios de la zona no saturada del suelo 6:91–98

Carballeira J, Pol C (1986) Características y evolución de los sedimentos lacustres miocenos de la región de Tordesillas (facies de las Cuestas) en el sector central de la Cuenca del Duero. Stvdia Geol Salmant 22:213–246

Carretero Rivera MC, Vega Alegre M, Pardo Almudí R, Fernández Pérez L, Barrado Esteban E, Del Barrio Beato V (2004) Posible origen y dispersión de Arsénico en los acuíferos de la zona de Vallelado-Mata de Cuéllar (Segovia). Proc III Simp Hidrogeol Zaragoza, Spain. Hidrogeol Rec Hidraul 26:677–687

Colmenero JR, Rodríguez M, Gómez JJ, Carrasco P (2001) Estratigrafía del subsuelo y evolución sedimentaria del sector sur de la cuenca terciaria del Duero. Geotemas 3:129–132

Confederación Hidrográfica del Duero (CHD) (2001a) Estudio de la contaminación de las aguas subterráneas por contenido de arsénico, pp 1–29

CHD (2001b) Asistencia Técnica Construcción de piezómetros y sondeos. Red de nitratos. Segunda Fase. Muestreo 1ª Campaña año 2000, pp 1–22

CHD (2001c) Asistencia Técnica Construcción de piezómetros y sondeos. Red de nitratos. Segunda Fase. Muestreo 2ª Campaña año 2000, pp 1–18

CHD (2002a) Asistencia Técnica Construcción de piezómetros y sondeos. Red de nitratos. Segunda Fase. Muestreo 1ª Campaña año 2001, pp 1–27

CHD (2002b) Asistencia Técnica Construcción de piezómetros y sondeos. Red de nitratos. Segunda Fase. Muestreo 2ª Campaña año 2001, pp 1–29

CHD (2003a) Asistencia Técnica Construcción de piezómetros y sondeos. Red de nitratos. Segunda Fase. Muestreo 1ª Campaña año 2002, pp 1–34

CHD (2003b) Asistencia Técnica Construcción de piezómetros y sondeos. Red de nitratos. Segunda Fase. Muestreo 2ª Campaña año 2002, pp 1–35

CHD (2003c) Red de nitratos. 3ª Fase. Campaña de muestreo y análisis mayo-junio 2003, pp 1–25

Corrochano A (1977) Estratigrafía y sedimentología del Paleógeno en la provincia de Zamora. PhD, University of Salamanca

Corrochano A (1982) Costras ferralíticas y unidad basal del Paleógeno en Zamora. Temas Geol Min 6:802–806

Corrochano A, Armenteros I (1989) Los sistemas lacustres neógenos de la cuenca terciaria del Duero. Acta Geol Hisp 24:259–279

Corrochano A, Fernández Macarro B, Recio C, Blanco JA, Valladares I (1986) Modelo sedimentario de los lagos neógenos de la Cuenca del Duero. Sector Centro-Oriental. Stvdia Geol Salmant 22:93–110

Duker AA, Carranza EJM, Hale M (2005) Arsenic geochemistry and health. Environ Int 31:631–641

Fernández García P, Mas R, Rodas M, Luque del Villar FJ, Garzón MG (1989) Los depósitos aluviales del paleógeno basal en el sector suroriental de la cuenca del Duero (provincia de Segovia): evolución y minerales de la arcilla característicos. Estud Geol 45:27–44

García-Sánchez A, Álvarez-Ayuso E (2003) Arsenic in soils and waters and its relation to geology and mining activities (Salamanca Province, Spain). J Geochem Explor 80:69–79

García-Sánchez A, Moyano A, Mayorga P (2005) High arsenic contents in groundwater in central Spain. Environ Geol 47(6):847–854

Gromet LP, Dymek RF, Haskin LA, Korotev RL (1984) The 'North American shale composite': its compilation, major and trace element characteristics. Geochim Cosmochim Acta 48:2469–2482

Gurung JK, Ishiga H, Khadka MS (2005) Geological and geochemical examination of arsenic contamination in groundwater in the Holocene Terai Basin, Nepal. Environ Geol 49:98–113

Hernández-García ME, Custodio E (2004) Natural baseline quality of Madrid Tertiary Detrital Aquifer groundwater (Spain): a basis for aquifer management. Environ Geol 46:173–188

Hernández García ME, Fernández Ruiz L (2002) Presencia de arsénico de origen natural en las aguas subterráneas del acuífero detrítico del Terciario de Madrid. Bol Geol Min 113:119–130

IGME-SGE (2004) Mapas Geológico y tectónico de España, a escala 1:2.000.000. In: Vera JA (ed) Geología de España. SEG-IGME, Madrid

Jiménez E (1973) El Paleógeno del borde SW de la Cuenca del Duero. II: La Falla de Alba-Villoria y sus implicaciones estratigráficas y geomorfológicas. Stvdia Geol Salmant 5:107–136

Jiménez E, Corrochano A, Alonso Gavilán A (1983) El Paleógeno de la Cuenca del Duero. In: Comba JA (ed) Libro Jubilar JM Ríos. Tomo II. Geología de España, IGME, pp 489–494

Korte N (1991) Naturally occurring arsenic in groundwater of the Midwest United States. Environ Geol Water Sci 18:137–141

Matschullat J, Ottenstein R, Reimann C (2000) Geochemical background—can we calculate it? Environ Geol 39(9):990–1000

Mediavilla R, Dabrio CJ, Martín-Serrano A, Santisteban JI (1996) Lacustrine systems of the Duero Basin: evolution and controls. In: Friend PF, Dabrio CJ (eds) Tertiary basins of Spain the stratigraphic record of crustal kinematics. Cambridge University Press, Cambridge, pp 228–236

Molina E, García Talegón J, Vicente MA (1997) Palaeoweathering profiles develop on the Iberian Hercynian Basement and their relationship to the oldest Tertiary surface in central and western Spain. In: Widdowson M (ed) Recognition, reconstruction and palaeoenvironmmental reconstruction, Special publication 120. Geological Society of London, London, pp 175–185

Moyano A, Mayorga P, García-Sánchez A (2002) Contaminación de Arsénico en aguas subterráneas de Castilla-León. Av Calidad Ambiental 27:451–455

Navarro A, Fernández Uría A, Doblas Domínguez JG (1989) Las aguas subterráneas en España. Estudio de síntesis. ITGE, Madrid, pp 1–591

Nriagu JO (ed) (1994) Arsenic in the environment. Part II: human health and ecosystem effects. Advances in environmental science and technology, Series 27. Wiley, New York, p 320

O'Neill P (1995) Arsenic. In: Alloway BJ (ed) Heavy metals in soils, Blackie Academic and Professional, London, pp 105–121

Oremland SS, Stolz JF (2003) The ecology of arsenic. Science 300:939–944

Pérez González A, Martín-Serrano A, Pol C (1994) Depresión del Duero. In: Gutiérrez Elorza M (ed) Geomorfología de España. Rueda, Madrid, pp 351–388

Pol C, Buscaloni A, Carballeira J, Frances V, López-Martínez N, Marandat B, Moratalla JJ, Sanz JL, Sige B, Villatte J (1992) Reptiles and mammals from the late Cretaceous new locality Quintanilla del Coco (Burgos province, Spain). Neues Jahrb Geol Palaontol Abh 143:279–314

Portero JM, del Olmo P, Ramírez J, Vargas I (1982) Síntesis del Terciario continental de la Cuenca del Duero. Temas Geol Min 6:11–40

Sahún B (1991) Estudio Hidrogeológico de la unidad hidrogeológica del Páramo de Cuellar (Segovia-Valladolid). Dirección General de Obras Hidráulicas, pp 1–44

Sahún B (2001) Normas de otorgamiento de concesiones de las unidades hidrogeológicas 02.13 Páramo de Cuéllar y 02.17 Región de los Arenales. Cuenca del Duero. Dirección General de Obras Hidráulicas y Calidad de las Aguas, pp 1–66

Sahún B (2002) Estudio del sistema de utilización conjunta de los recursos hídricos superficiales y subterráneos de las cuencas del Cega-Pirón y Adaja-Eresma. Dirección General de Obras Hidráulicas, pp 1–123

Sahún B, Niñerola S, Gómez JJ, Lillo J, del Olmo P, Hernández A (2003) Estudio del contenido de arsénico en la zona central de la Depresión del Duero. Dirección General de Obras Hidráulicas y Calidad de las Aguas, pp 1–192

Sahún B, Gómez JJ, Lillo J, Olmo P (2004a) Arsénico en aguas subterráneas e interacción agua-roca: un ejemplo en la cuenca terciaria del Duero (Castilla y León, España). Rev Soc Geol Esp 17:137–155

Sahún B, Gómez JJ, Lillo J (2004b) Arsenic in groundwaters and rocks in the Duero Tertiary Basin (Central Spain). In: Proceedings of the 32nd international geological congress, Florence, 2004. Session T38.03—Groundwater resource problems in the Mediterranean area: quantity and quality. 80–16 Booth 527

Sánchez A, Delgado C, García-Hernán O, Sahún B, Ballester A (1990) Cuenca del Duero. In: Sánchez A (ed) Unidades hidrogeológicas de la España peninsular e Islas Baleares. Servicio Geológico, Ministerio de Obras Públicas y Urbanismo, Madrid. Informaciones y estudios 52:1–32

Santisteban JI, Martín-Serrano A (1991) El Paleógeno del sector surocidental de la Cuenca del Duero: Nueva división estratigráfica y controles sobre su sedimentación. In: Colombo F (ed) Libro homenaje a Oriol Riba. Acta Geol Hisp 26:133–148

Santisteban JI, Mediavilla R, Martín-Serrano A, Dabrio CJ (1996a) The Duero Basin: a general overview. In: Friend PF, Dabrio CJ (eds) Tertiary basins of Spain the stratigraphic record of crustal kinematics. Cambridge University Press, Cambridge, pp 183–187

Santisteban JI, Mediavilla R, Martín-Serrano A (1996b) Alpine tectonic framework of south-western Duero basin. In: Friend PF, Dabrio CJ (eds) Tertiary basins of Spain the stratigraphic record of crustal kinematics. Cambridge University Press, Cambridge, pp 188–195

Schreiber ME, Simo JA, Freiberg PG (2000) Stratigraphic and geochemical controls on naturally occurring arsenic in groundwater, eastern Wisconsin, USA. Hydrogeol J 8:161–176

Schreiber ME, Gotkowitz MB, Simo JA, Freiberg PG (2003) Mechanism of arsenic release to ground water from naturally occurring sources, eastern Wisconsin. In: Welch AH, Stollenwerk KG (eds) Arsenic in ground water. Kluwer, Boston, pp 260–280

Smedley PL, Kinninburgh DG (2002) A review of the source, behaviour and distribution of arsenic in natural waters. Appl Geochem 17:517–568

Stollenwerk KG (2003) Geochemical processes controlling transport of arsenic in groundwater: a review of adsorption. In: Welch AH, Stollenwerk KG (eds) Arsenic in ground water. Kluwer, Boston, pp 68–100

Welch AH, Westjohn DB, Helsel DR, Wanty RB (2000) Arsenic in groundwater of the United States: occurrence and geochemistry. Ground Water 38:589–604